EJN fens EUROPEAN JOURNAL OF NEUROSCIENCE

European Journal of Neuroscience, Vol. 33, pp. 9–25, 2011 doi:10.1111/j.1460-9568.2010.07477.x

MOLECULAR AND DEVELOPMENTAL NEUROSCIENCE

Metamorphosis and the regenerative capacity of spinal cord axons in *Xenopus laevis*

Kurt M. Gibbs,[1] Sridar V. Chittur[2] and Ben G. Szaro[1]

[1]Department of Biological Sciences and the Center for Neuroscience Research, University at Albany, State University of New York, 1400 Washington Avenue, Albany, NY 12222, USA

[2]Center for Functional Genomics and Department of Biomedical Sciences, University at Albany, State University of New York, Rensselaer, NY, USA

Keywords: axon regeneration, microarray, spinal cord injury, thyroid hormone

Abstract

Throughout the vertebrate subphylum, the regenerative potential of central nervous system axons is greatest in embryonic stages and declines as development progresses. For example, *Xenopus laevis* can functionally recover from complete transection of the spinal cord as a tadpole but is unable to do so after metamorphosing into a frog. Neurons of the reticular formation and raphe nucleus are among those that regenerate axons most reliably in tadpole and that lose this ability after metamorphosis. To identify molecular factors associated with the success and failure of spinal cord axon regeneration, we pharmacologically manipulated thyroid hormone (TH) levels using methimazole or triiodothyronine, to either keep tadpoles in a permanently larval state or induce precocious metamorphosis, respectively. Following complete spinal cord transection, serotonergic axons crossed the lesion site and tadpole swimming ability was restored when metamorphosis was inhibited, but these events failed to occur when metamorphosis was prematurely induced. Thus, the metamorphic events controlled by TH led directly to the loss of regenerative potential. Microarray analysis identified changes in hindbrain gene expression that accompanied regeneration-permissive and -inhibitory conditions, including many genes in the permissive condition that have been previously associated with axon outgrowth and neuroprotection. These data demonstrate that changes in gene expression occur within regenerating neurons in response to axotomy under regeneration-permissive conditions in which normal development has been suspended, and they identify candidate genes for future studies of how central nervous system axons can successfully regenerate in some vertebrates.

Introduction

The capacity for functional recovery from spinal cord injury varies phylogenetically across the vertebrate subphylum. Amniotes generally lose this capacity during fetal development, whereas anamniotes such as lamprey and salamander fully recover throughout life. In anurans, however, the loss of spinal cord regenerative capacity occurs at metamorphosis (Sims, 1962; Forehand & Farel, 1982; Beattie *et al.*, 1990; Ten Donkelaar, 2000). This precise temporal correlation makes tadpoles an attractive model system for studying the underlying cellular and molecular bases for the developmental loss of regenerative capacity.

The observation that tadpoles that spontaneously fail to metamorphose also fail to recover from spinal cord injury has led to speculations that metamorphosis itself may be required for recovery (Beattie *et al.*, 1990). During anuran metamorphosis, which is controlled by steadily rising levels of thyroid hormone (TH), the transition from swimming to limb-based locomotion is mediated by extensive cellular proliferation and rewiring of the nervous system (Marsh-Armstrong *et al.*, 2004). Such rewiring could effect recovery simply by bypassing damaged connections. Yet, double labeling of cut axons with fluorescent dextran amines has shown that regeneration of severed spinal cord axons, particularly those of reticular and raphe neurons, occurs in *Xenopus* tadpoles (Gibbs & Szaro, 2006). Because these projections are essential for voluntary movement, recovery of function does involve regeneration of cut axons. Premetamorphic tadpoles subjected to spinal cord injury typically recover during metamorphosis, making the parsing of the cellular and molecular events of regeneration and recovery from those of metamorphosis problematic. The possibility remains that metamorphosis is necessary to create conditions that promote regeneration.

To begin to separate cellular and molecular mechanisms relevant to regeneration from those of metamorphosis, levels of TH were pharmacologically manipulated in *Xenopus laevis* tadpoles subjected to complete spinal cord transection prior to the onset of endogenous TH production. In *Xenopus*, the transition from larval to juvenile forms is controlled directly by steadily rising levels of TH, from the onset of prometamorphosis at stage 54 through metamorphic climax at stage 61 (Gudernatsch, 1912; Dodd & Dodd, 1976; Leloup and Buscaglia, 1977; Tata, 2006). These rising levels of TH initiate transcription of immediate response genes at varying thresholds in

Correspondence: Ben G. Szaro, as above.
E-mail: bgs86@albany.edu

Received 25 May 2010, accepted 17 September 2010

each responding tissue. The expression of these TH-responsive genes in turn induces that of multiple downstream genes specific to each cell type (Shi, 2000). The entire cascade can be inhibited effectively by methimazole treatment (Buckbinder & Brown, 1993), which blocks endogenous TH synthesis; such treatment of pre-metamorphic tadpoles arrests development at stage 54. Alternatively, treating them with 3,3′,5-triiodo-L-thyronine (T3) prematurely accelerates their development toward metamorphic climax (Buckbinder & Brown, 1993; Brown *et al.*, 1995; Shi, 2000, 2009; Brown & Cai, 2007). Using these established pharmacological paradigms, we asked whether growth of axons across a spinal cord lesion and functional recovery occur if metamorphosis is inhibited or prematurely induced. This paradigm was also used to suppress the high background of changes in gene expression taking place during metamorphosis to identify specific changes in gene expression in hindbrain that accompany successful axon regeneration.

Materials and methods

Animals

Pre-metamorphic tadpoles (Nieuwkoop and Faber stages 51–53; Nieuwkoop & Faber, 1994) and juvenile frogs (2 weeks post-metamorphic) were periodic albino *Xenopus laevis* (Hoperskaya, 1975; Tompkins, 1977) obtained from our breeding colony at the State University of New York at Albany. Tadpoles and juveniles were maintained at 24 °C on a diet of suspended nettle powder (Wunderlich-Diez, Milburn, NJ) and at 21 °C on a diet of salmon chow (Rangen, Buhl, ID, USA), respectively. Procedures in this study were approved by the Institutional Animal Care and Use Committee (IACUC) of the State University of New York at Albany.

Spinal cord transection and pharmacological manipulation of TH levels

Tadpoles and juvenile frogs were anesthetized by immersion in 0.04 and 0.1%, respectively, ethyl 3-aminobenzoate methanesulfonate (MS-222; Sigma-Aldrich, St Louis, MO, USA). Fully anesthetized animals were placed into a beeswax-lined petri dish, where they were restrained with rubber bands anchored by straight pins. A dorsolateral incision at the mid-thoracic level was made using Vannas-style microdissecting spring scissors (15000-00; Fine Science Tools, Foster City, CA, USA) to cut through the skin, some axial musculature, and cartilaginous vertebrae. The spinal cord was then completely transected with the microdissecting scissors. The totality of the lesion was confirmed at the time of surgery by passing the tips of fine forceps (modified Dumont #5 Biologie tips; Fine Science Tools) through the injury site while observing the spinal cord; this was possible because periodic albino tadpoles lack pigment and are largely transparent. For further confirmation that the transections were complete, we examined the behavior of the animals 1 day after surgery for signs of residual movement; any animals showing such signs were removed from the study. Animals were post-operatively maintained in individual 1.5-L tanks filled with aerated sterile-filtered tap water containing 4 mg/L gentamicin sulfate (Sigma-Aldrich).

For the methimazole-treated groups, tadpoles were placed in water containing 1 mM methimazole (M8506; Sigma-Aldrich) 3 days prior to the operation to ensure that TH production was inhibited by the time of the surgery. After surgery, both the methimazole- and T3-treated groups were maintained continuously in rearing water containing, respectively, 1 mM methimazole or 5 nM T3 (T6397; Sigma-Aldrich); rearing water was changed daily.

Immunohistochemistry

Animals were killed with an overdose of MS-222, and the central nervous system (CNS) encased in its vertebral column was dissected free and immersion-fixed overnight in phosphate-buffered (0.1 M sodium phosphate, pH 7.4) 10% formalin (PB-formalin). To remove the fixative and protect them from freeze damage, tissues were immersed successively overnight in PB and then in 30% sucrose in PB. Prior to further processing, the CNS was photographed as a whole mount through a stereomicroscope (Leica MZ16 FA). The brain and spinal cord were then embedded in Tissue Freezing Medium (Triangle Biomedical, Durham, NC, USA) and cryosectioned at 20 μm either parasagittally or transversely. Sections were thaw-mounted onto gelatin-coated glass slides, post-fixed in PB-formalin, and processed for double-label immunofluorescence.

For immunohistochemistry, washes were done in Tris–buffered saline (TBS; 50 mM Tris, 150 mM NaCl, pH 7.5), and blocking of nonspecific binding of antibodies was done in 10% fetal calf serum (2 h), followed by 5% bovine serum albumin (BSA) and 3% normal serum in TBS (1 h) at room temperature. Immunostaining with each primary and secondary antibody was done overnight at 4 °C, and slides were mounted under cover glass with Fluoromount-G (SouthernBiotech, Birmingham, AL, USA). The secondary antibodies used to detect the middle neurofilament protein (NF-M), serotonin and brain lipid binding protein (BLBP) primary antibodies were Alexafluor 488 goat antimouse, Alexafluor 546 goat antirat and Alexafluor 546 goat antirabbit (Molecular Probes, Eugene, OR, USA), respectively, at a concentration of 2 μg/mL and an incubation period of 2–4 h. Immunostained slides were imaged using a Zeiss LSM 510 Meta laser scanning confocal microscope. The objectives and scanning parameters used for each image are provided in the figure legends.

For assays of the extent of reinnervation of the lesion site, confocal images of NF-M-immunostained parasagittal sections were imported as tiff files into Metamorph (version 7.6). For each section, the density of immunofluorescence (total integrated immunofluorescence intensity divided by the pixel area) was determined for the region of interest, as defined by the ventral tissue bridge spanning the lesion site. These values were then normalized to the density of NF-M immunofluorescence within the ventral tract of unoperated controls and averaged among animals for each treatment and timepoint. Statistical pairwise comparisons were then performed using *t*-tests, with the degrees of freedom determined by the number of animals used in the comparisons (Sachs, 1984).

Antibody characterization

The mouse monoclonal antibody RMO270 (2 μg/mL) was used to label axons. This antibody, which is an IgG2a, targets the *Xenopus* NF-M independently of its state of phosphorylation (Szaro *et al.*, 1989; Wetzel *et al.*, 1989). It was originally made against rat neurofilaments and recognizes an epitope at the C-terminus of NF-M that is conserved from torpedo fish to human and is found in *Xenopus* (Shaw, 1992; Gervasi & Szaro, 1997). It has been used extensively in immunohistochemical studies in *Xenopus* to label developing and regenerating axons from early neurulae stages through metamorphosis (Lin & Szaro, 1994; Zhao & Szaro, 1994; Undamatla & Szaro, 2001).

Serotonergic axons were labeled with a rat monoclonal antibody (clone YC5/45, diluted 1 : 100; GTX26336, GeneTex, Irvine, CA, USA) that targets serotonin (Consolazione *et al.*, 1981; Milstein *et al.*, 1983). This antibody was raised against a serotonin–bovine serum

albumin immunogen and has been shown in aldehyde-fixed tissue sections to react with serotonergic but not dopaminergic neurons, and to lose immunoreactivity when serotonin synthesis is suppressed (Consolazione *et al.*, 1981; Milstein *et al.*, 1983).

BLBP was detected with a rabbit antiserum (1 : 1000) raised against the full length (132 amino acid) mouse recombinant protein expressed in *E. coli* (Feng *et al.*, 1994). In mouse developing cerebellum, the antibody stains Bergmann glia during the period of neuronal differentiation and migration and recognizes a single 15-kDa band on Western blots. Expression of BLBP in subsets of radial glia is conserved in other vertebrates including zebrafish (Raymond *et al.*, 2006) and turtle (Rehermann *et al.*, 2009). *Xenopus laevis* expresses a highly similar protein (Fabp7; accession number NM_001095326) of the same length and which is 82% identical (91% similar) to the mouse protein and, in *Xenopus* spinal cord, the antibody stains cells morphologically resembling GFAP- and vimentin-positive radial glia (Szaro & Gainer, 1988).

In situ *hybridization*

Tadpoles (five per group) that underwent no drug treatments received spinal cord transections as described above and were allowed to recover for 1, 3 days or 1 week. An equal number of age-matched unoperated animals were selected for each timepoint to be used as controls. The dissected CNS was prepared for cryosectioning as described for immunocytochemistry except that sections were thaw-mounted onto silane-coated slides (Polysciences Inc.). GAP-43 cDNA was obtained by PCR from cDNA prepared from *Xenopus laevis* spinal cord (forward primer ATAAT GGATC CTGAT GATCA GCACA GACAG AGCTC A; reverse primer ATTAA GGATC CCAAA CTGTC GGGAG GGCTA TTTGT T) and subsequently subcloned into a pGEM3Z (Promega) RNA-expression plasmid. The preparation of *Xenopus* NF-M and peripherin cDNAs, as well as methods for *in vitro* transcription of digoxigenin-labeled cRNA probes, hybridization, and visualization using alkaline phosphatase-conjugated antibodies to digoxigenin, were as described elsewhere (Gervasi *et al.*, 2003).

Behavioral testing

Tadpoles from each of three groups (methimazole, $n = 14$; T3, $n = 18$; and untreated, $n = 3$) were scored independently by two investigators the day after surgery and then on a weekly basis for the following behaviors: startle reflex, volitional swimming, fictive swimming and righting reflex (Beattie *et al.*, 1990). The startle reflex, which is an involuntary response to noise resulting in the animal swimming away from the source, was elicited by sharply striking the side of the recovery tank once with a pencil. Volitional swimming is the tadpole's voluntary use of tail undulation in a straight or circular stroke pattern to move in a particular direction. Fictive swimming is movement of the distal tail while hovering or floating to stay in place. The righting reflex is the ability of the tadpole to maintain its correct posture (dorsal side up) when swimming or floating. Behaviors were scored as 1 (absent), 2 (weakly present), or 3 (moderately present to normal) for each animal and then tabulated as the mean (± SEM) score for animals in that group.

Gene expression profiling of hindbrain by microarray

Premetamorphic (NF stage 51–53) tadpoles receiving spinal cord transections were subsequently treated with either 1 mM methimazole for 3 days, 1 or 3 weeks, or with T3 for 3 days or 1 week. Unoperated animals treated with methimazole for 1 week served as a reference control for statistical comparisons against each experimental group. Animals were killed with an overdose of MS-222, and the CNS encased in its vertebral column was quickly removed and placed into RNA*later* (Ambion, Austin, TX, USA) for 1 h at room temperature. The CNS was later dissected free, and the hindbrain was harvested between the rostral and caudal margins of the fourth ventricle. The tissue was then homogenized (Polytron, Kinematica, Inc., Bohemia, NY), and total RNA was extracted (RNeasy Plus Mini kit; Qiagen, Valencia, CA, USA). For each individual hindbrain sample (90 total), the integrity of the RNA was assessed using Bioanalyzer Pico Chips (Agilent Technologies, Santa Clara, CA, USA). For each of the six treatment groups (15 animals each), three biological replicates were created for each group by pooling equal amounts of total RNA from five animals. Total RNA was then amplified and labeled using the One Cycle Amplification kit (Affymetrix, Santa Clara, CA, USA). The RNA was then fragmented and hybridized onto Affymetrix *Xenopus laevis* 2.0 microarrays at the Center for Functional Genomics (University at Albany, State University of New York, Rensselaer, NY, USA). Affymetrix Poly-A RNA and hybridization controls were added to samples to ensure the quality of amplification and hybridization, respectively.

Subsequent data analysis was performed using GENESPRING GX 10 Software (Agilent). In applying the MAS 5.0 algorithm, the methimazole-treated unoperated condition was used as the baseline for pairwise comparisons against each of the other five conditions. Data were further filtered by: (i) rejecting probe sets marked absent in all conditions; (ii) removing genes whose expression fell into the bottom 20th percentile of all conditions; (iii) selecting genes that showed differential expression at or above 1.8-fold; and (iv) using $P < 0.05$ as the criterion for significance in a nondirectional *t*-test (treatment vs. methimazole-treated, unoperated control).

Whenever possible, the UniGene ID (http://www.ncbi.nlm.nih.gov/unigene), which is used by Affymetrix to designate each transcript on the array, was used to assign the gene name. When no name was given in the UniGene entry, a prospective name was assigned using the most probable identification derived from BLASTing the UniGene ID sequence using the BLink tool in UniGene. The latter are identified in the Tables by the abbreviations HP (hypothetical protein) or MGC (mammalian gene collection) within the gene name. The functional category of individual genes was obtained through GeneCards (http://www.genecards.org).

Array validation

Fifteen genes were selected for validation spanning the range of significant fold-changes from low (1.8-fold) to high (13.6-fold). These were quantified by quantitative real-time reverse transcriptase polymerase chain reaction (qRT-PCR) from the same pools of total RNA that were used on the arrays. Total RNA was reverse-transcribed with oligo dT primers and Super Script III reverse transcriptase (Invitrogen) to generate cDNA. Power Sybr Green master mix (Applied Biosystems) was then used following the protocol of the manufacturer with primers that amplified a 150–200 base-pair amplicon. Fold changes were determined using the $\Delta\Delta C_T$ method (Livak & Schmittgen, 2001), normalizing to 18S rRNA, the expression of which was highly constant in both the microarray and qRT-PCR results. Results were averaged among the three groups of pooled animals for each condition.

Statistical analysis

Data are expressed as mean ± SEM. For comparison of the density of NF-M immunostaining within the tissue bridge across the lesion site, a

directional Student's *t*-test was performed between no drug treatment and methimazole treatment vs. T3 treatment, with degrees of freedom determined by the number of animals (Fig. 3). For behavioral data (Fig. 6), pairwise nondirectional comparisons were made among the no drug, methimazole- and T3-treated groups for each timepoint using the Wilcoxon, Mann and Whitney *U*-test, a nonparametric test for ranked data. For microarray data (Tables 2–4; Fig. 7), a nondirectional Student's *t*-test was performed between treatment and the methimazole-treated unoperated control, with degrees of freedom determined by the number of arrays. Calculations for immunohistochemical and behavioral data were performed using a hand-held calculator in conjunction with published formulae and tables (Sachs, 1984). Calculations for array data were done using GENESPRING GX 10 software** (Agilent). Results were considered statistically significant at $P \leq 0.05$.

Results

Effects of methimazole and T3 on normal development

To manipulate TH levels and their effects on development, we followed well-established pharmacological paradigms for the use of methimazole and T3 in *Xenopus laevis* (Buckbinder & Brown, 1993). In *X. laevis*, endogenous TH production begins at NF stage 54, gradually peaking at metamorphic climax (NF stage 61) and declining thereafter (Leloup and Buscaglia, 1977; Simon *et al.*, 2002). Prior to the production of endogenous TH, animals develop without the need for the hormone, successfully reaching stages that include the eruption and pattern formation of both fore- and hindlimbs (Shi, 2000). Rising levels of TH drive subsequent development, including maturation and innervation of the limbs, as well as considerable neuro- and gliogenesis in the CNS (Marsh-Armstrong *et al.*, 2004).

Confirmatory of these earlier observations, methimazole treatment of stage 51–53 tadpoles effectively arrested development at stage 54 (Fig. 1C). Such tadpoles were essentially indistinguishable from untreated stage 53–54 tadpoles (Fig. 1A). Conversely, T3 treatment at these stages accelerated tadpole development markedly (compare B and D in Fig. 1). Within 1 week of the onset of T3 treatment, growth and differentiation of the hindlimbs were greatly accelerated. In addition, the eyes, brain and head underwent a near complete transformation from the morphology typically associated with tadpoles to that associated with froglets. Continuous exposure of tadpoles to 5 nM T3 unfortunately led to asynchronous development and poor survival beyond 1 week, necessitating their killing at this time.

Effects of TH on wound healing

Differences among the various treatments in the reconstitution and wound healing of transected spinal cord were visible under external examination (Fig. 2). One week after transection, reconstitution of the cut spinal cord was similarly incomplete in untreated tadpoles and those treated with methimazole. Ventrally the cut ends appeared rejoined but dorsally they remained separate to varying degrees. At 3 weeks, healing of untreated animals had progressed much further than it did with methimazole treatment. In the untreated animals, the cut ends had completely rejoined and, except for the dorsal fissure deviating from the midline, the wound was nearly invisible. With methimazole treatment the wound site remained visible, forming a line of constriction that circumscribed the spinal cord. With T3 treatment

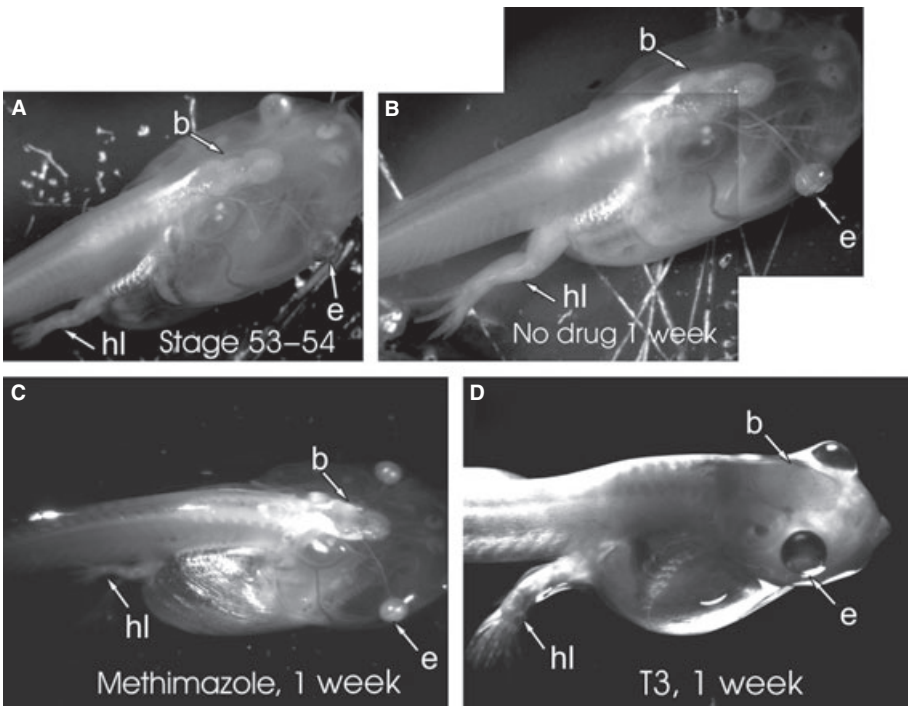

FIG. 1. Effects of altering TH levels on normal development. (A) Untreated late stage 53 tadpole. (B) The same tadpole as in A, 1 week later, without drug treatment. (C) Tadpole treated with 1 mM methimazole from late stage 53 onward for 1 week, to block endogenous TH synthesis prior to its normal onset. (D) Tadpole treated with 5 nM T3 from late stage 53 onward for 1 week to bring TH levels prematurely to levels similar to those experienced at metamorphic climax. With methimazole treatment, development progresses only as far as NF stage 54, whereas with T3 treatment, anatomical features typically seen only at late metamorphic climax (after stage 60) appear prematurely. Note especially the relative appearance of the hindlimb (hl), brain (b), eye (e) and head (h) between the two treatments.

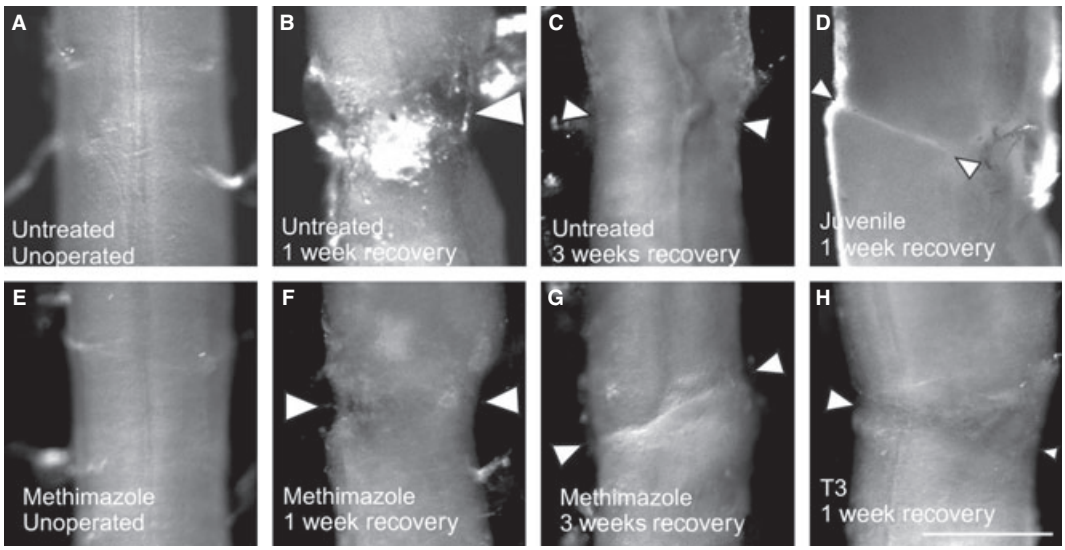

FIG. 2. Effects of altering TH levels on wound healing after spinal cord transection. (A–C and E–H) *Xenopus laevis* tadpoles (NF stage 51–53) or (D) juvenile frogs received a complete spinal cord transection and were allowed to recover for 1 (B, D, F and H) or 3 (C and G) weeks before killing. After fixation, spinal cords were dissected free and imaged through a dissecting microscope (Leica MZ16FA). At 1 week, wound healing (arrowheads) was similar in (B) untreated and (F) methimazole-treated tadpoles; rostral (top) and caudal (bottom) spinal cord segments were not yet completely healed together. (C and G) At 3 weeks, the separated segments had completely rejoined; the wound (arrowheads) was nearly indiscernible in untreated tadpoles (C), but was more evident in those treated with methimazole (G). (H) With 5 nM T3 treatment at 1 week, wound healing was more advanced than in either methimazole-treated or untreated tadpoles at the same time point. The rostral (above the arrowheads) and caudal (below the arrowheads) segments of transected T3-treated spinal cord were joined by a translucent cuff of tissue. (D) In untreated juvenile frogs, 1 week after transection, the rostral (top) and caudal (bottom) segments were also joined together, but the ends of the segments were separated by a sharper boundary than in the other cases (arrowheads). Scale bar, 1 mm (applies to all panels).

and in untreated juveniles, at 1 week, wound healing appeared distinctly different from that of either untreated or methimazole-treated tadpoles at the same timepoint. Although the cut ends had largely rejoined in T3-treated tadpoles, the juncture appeared as a translucent cuff of tissue surrounding the spinal cord which, based on the histological evidence presented next, appeared to be the result of regrowth of meninges rather than of axons. In untreated juveniles, the transection site formed a sharply constricted boundary, resembling the early stages of scar formation reported by others (Beattie *et al.*, 1990).

Effects of TH on axon regeneration

For both untreated and methimazole-treated tadpoles, histological examination of parasagittal sections confirmed that, within 1 week, the cut ends of the transected spinal cord had rejoined along the ventral aspect but remained separated dorsally (Fig. 3A and B). As revealed by immunostaining for NF-M, axons were evident throughout the reformed ventral tract of untreated tadpoles at 1 week (Fig. 3A). Axons were also visible crossing the lesion site of methimazole-treated tadpoles (Fig. 3B), but they were less dense than in untreated tadpoles. At 3 weeks, NF-M-immunostained axons were more abundant within the lesion site of both groups (Fig. 3D and E), although staining still appeared more pronounced in untreated than in methimazole-treated animals. In sharp contrast, axons of T3-treated tadpoles and juvenile froglets at 1 week approached but did not appreciably invade the lesion site (Fig. 3C and F).

One way to quantify reinnervation is to analyze the intensity of neurofilament immunostaining across a lesion, as has been done to estimate the degree of reinnervation following spinal cord injury in N-CAM-deficient transgenic mice (Zhang *et al.*, 2010). Thus, a comparison was made among these groups of the average intensity per unit area of NF-M immunofluorescence within the tissue bridge crossing the lesion site (integrated immunofluorescence intensity divided by area of the region of interest), normalized to that of the ventral tract of unoperated controls. These data confirmed what was seen by eye (Fig. 3G). At 1 week, the densities of NF-M immunofluorescence of the no drug treatment and methimazole-treated groups were 34 ± 9% and 22 ± 2% of that of unoperated control animals, respectively. These values were signficantly greater than that of T3-treated tadpole [$P = 0.04$ ($t_{2,2}$); $P = 0.001$ ($t_{3,2}$), respectively], at 6 ± 1%. At 3 weeks, the density of reinnervation as assayed in this way rose to 57% and 31 ± 6% of unoperated controls for the no drug and methimazole-treated animals, respectively. Collectively, these data indicated that axons regrew through the lesion in both methimazole-treated and in untreated tadpoles, but failed to do so in either T3-treated tadpoles or untreated juveniles. An antibody to serotonin was used in double-labeling experiments with the NF-M antibody to label specifically the descending axons of raphe and reticular neurons (Fig. 4). In *Xenopus,* these axons constitute the principal serotonergic axons of descending pathways (van Mier *et al.*, 1986) and have been demonstrated by double-labeling with fluorescent dextran amines to regenerate following spinal cord transection in tadpoles (Beattie *et al.*, 1990; Gibbs & Szaro, 2006). Because these hindbrain neurons are born before stage 51–53, the presence of serotonergic axons in the ventral tract has been taken as reliable evidence of successful regeneration of their axons (Beattie *et al.*, 1990; Ten Donkelaar, 2000). Although both serotonin and NF-M staining were visible in untreated and methimazole-treated tadpoles at 1 and 3 weeks, their colocalization was relatively rare (not shown). This may be because NF-M immunostaining may lag behind the tips of individual regenerating fibers, as reported in *Xenopus* regenerating optic nerve (Zhao & Szaro, 1994). Similarly, the vesicular nature of serotonin immunostaining makes it more difficult to assign labeling to individual axons unless NF-M staining is present. The colocalization of serotonin and NF-M became convincing at later timepoints. At 5 weeks after transection, for example, numerous axons that were

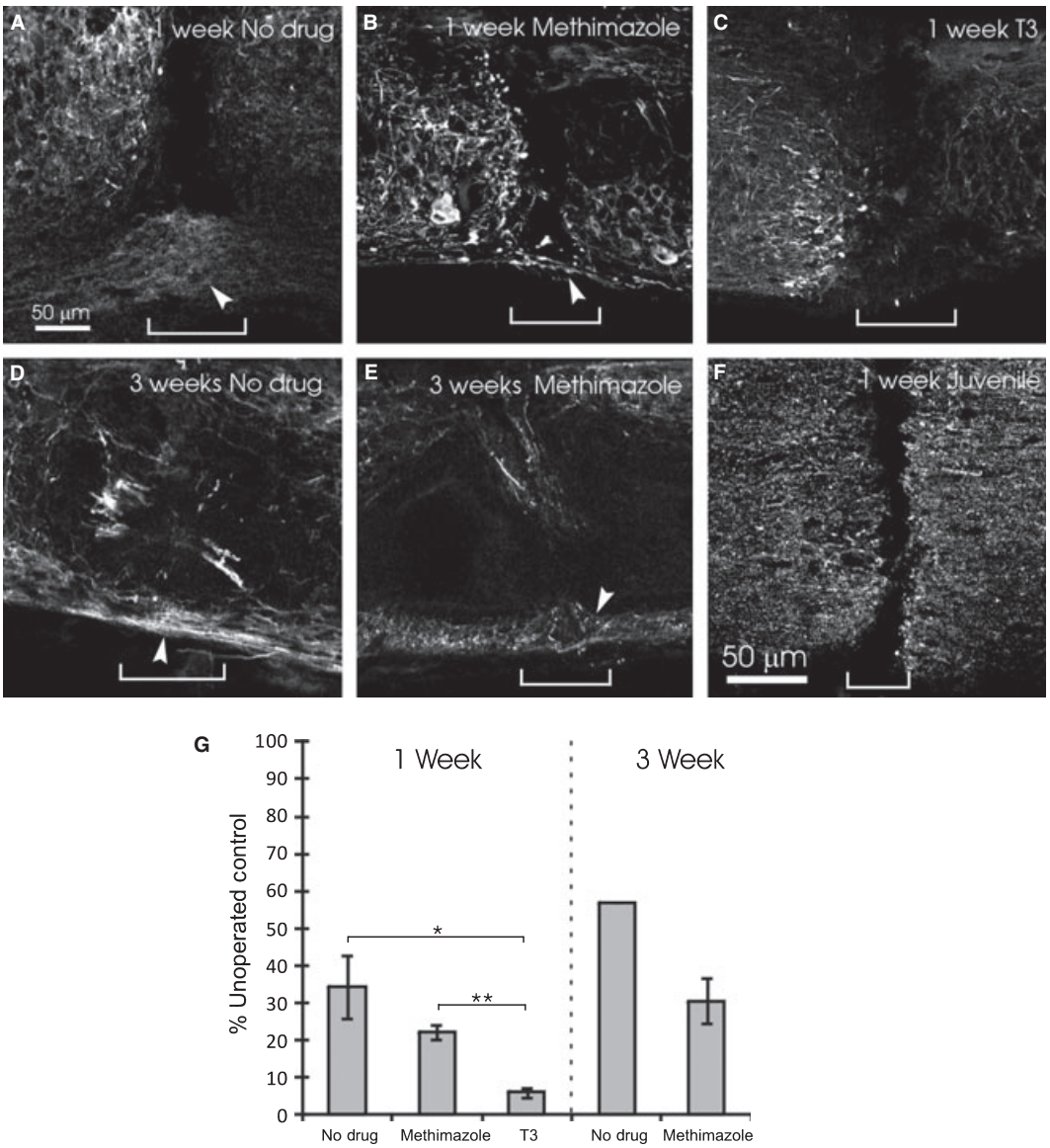

FIG. 3. The influence of TH on the ability of cut spinal cord axons to grow across the lesion. (A–C and F) One and (D and E) 3 weeks following complete spinal cord transection, parasagittal spinal cord sections were immunostained for NF-M. NF-M-positive axons (arrowheads) were seen crossing the injury site (horizontal bracket) in the ventral spinal cord of tadpoles receiving either no drug treatment (A and D) or 1 mM methimazole (B and E) but not in those treated with T3 (C) or in juvenile frog (F). Dorsal is up and rostral is to the left in all panels. Images represent a single optical section [20 ×, 0.75 NA; 0.9, 0.9, 2.1 μm (x, y, z)]. (G) Quantitative comparison of the density of NF-M immunostaining within the ventral tissue bridge crossing the lesion (integrated intensity of NF-M immunostaining within the tissue bridge divided by area of the tissue bridge), expressed as a percentage of that within the ventral tract of unoperated control tadpoles. *P = 0.04, ($t_{2,2}$); **P = 0.001 ($t_{3,2}$). Scale bar in A applies to A–E.

double-labeled for NF-M and serotonin were readily apparent in the descending tract of methimazole-treated animals subjected to spinal cord transection (Fig. 4), further confirming that the axons crossing the lesion had originated from the raphe and reticular nuclei and had thus regenerated in the absence of metamorphosis.

BLBP expression and axonal pathfinding in transected spinal cord

Radial glia bridge the gap in transected spinal cord in a variety of species, including *Xenopus* and newt, and regrowing axons appear to use them to facilitate crossing the lesion site (Michel & Reier, 1979; Singer *et al.*, 1979). An antibody against BLBP, which specifically labels radial glia (Feng *et al.*, 1994), has been used in turtle to label the glial tracks that axons use as they regrow (Rehermann *et al.*, 2009). Thus, we used this antibody to examine the degree to which TH affects the presence of BLBP-positive radial glial fibers and their ability to facilitate axon regeneration in *Xenopus*.

At 1 week post-surgery, BLBP-positive processes extensively bridged the lesion site of animals of all treatment groups (Fig. 5). However, consistent with differences in wound healing, BLBP processes filled in the lesion site more effectively in untreated and T3-treated tadpoles than in those treated with methimazole (compare Fig. 5A′, C′ and B′, respectively). Despite the presence of BLBP-positive radial glial fibers in all groups, NF-M-positive axons that invaded the lesion site appeared to co-localize generally with BLBP-positive fibers in only the untreated (Fig. 5A) and methimazole-treated (Fig. 5C) groups, consistent with the observation from other systems

that successfully regenerating axons use these radial glia to bridge the lesion site. With T3 treatment (Fig. 5C), BLBP-positive fibers within the lesion were not associated with NF-M-positive axons.

Behavioral recovery

To address whether animals recover function when metamorphosis is arrested, we tracked the recovery of functional behaviors in methimazole-treated animals ($n = 14$) on a weekly basis for 3 weeks. Earlier studies charting functional recovery of untreated animals found that behaviors return in a stereotypical pattern after complete spinal cord transection (Beattie *et al.*, 1990). The startle reflex returns first, followed by the restoration of volitional swimming, fictive swimming and the righting reflex, in that order. Our findings with untreated tadpoles confirmed these earlier studies – the startle reflex, as well as volitional and fictive swimming, began to return in untreated tadpoles by 1 week and were essentially normal by 2 weeks (Fig. 6). The righting reflex took the longest to recover; even at 3 weeks, tadpoles in the untreated group generally floated dorsal side down, only righting themselves while swimming.

Methimazole-treated animals also recovered function. Recovery of the startle reflex, a strong indicator of functional regeneration of ascending and descending pathways in anamniotic spinal cord (Zottoli & Freemer, 2006; Takeda *et al.*, 2007), was virtually as rapid in methimazole-treated tadpoles as in those without drug treatment; both groups were essentially normal with respect to this behavior at 2 weeks. The recovery of other behaviors occurred more slowly in methimazole-treated than in untreated tadpoles, consistent with the reduced staining of axons crossing the lesion site of methimazole-treated animals. Scores for volitional swimming in the methimazole-treated group were significantly lower than in the untreated group at 1 week (Wilcoxon–Mann–Whitney *U*-test; $0.02 < P < 0.05$), and those for fictive swimming at 2 weeks (Wilcoxon–Mann–Whitney *U*-test; $0.01 < P < 0.02$). Both these behaviors eventually recovered to normal at 5–6 weeks (not tabulated) but the righting reflex never recovered, suggesting that the return of this reflex requires normal development.

Over the 1-week period for which T3-treated animals ($n = 18$) could be followed, virtually every animal remained in their post-operative paralyzed state. Taken together with the morphological data, the behavioral data further supported the conclusion that, when prometamorphosis was arrested, axons were able to regenerate and restore function. No such recovery was seen in animals when precocious metamorphosis was invoked by T3 treatment.

Gene expression profiling of the hindbrain after spinal cord transection

Methimazole treatment allowed for the profiling of changes in gene expression during successful recovery from spinal cord injury while suppressing the considerable background of changes that accompany metamorphosis. For these studies, we decided to concentrate on changes in hindbrain, the source of regenerating spinal cord axons, rather than at the injury site, to characterize changes occurring in the cells of origin of regenerating axons. The RNAs analyzed on microarrays came from the hindbrains of six separate groups of animals: (i) unoperated, methimazole-treated stage 51–53 tadpoles (reference control); (ii–iv) methimazole-treated, spinal cord-transected animals at 3 days, 1 and 3 weeks (regeneration-permissive conditions); and (v and vi) T3-treated, spinal cord-transected animals at 3 days and 1 week (regeneration-inhibitory conditions). Employing stringent filtering criteria (see Materials and methods), we identified genes from each group whose expression changed significantly relative to the unoperated, methimazole-treated, reference control group. In total, 202, 331 and 275 transcripts [which included expressed sequence tags (ESTs) as well as annotated and prospective genes] were identified as differentially expressed from the 3-day, 1-week and 3-week timepoints of the methimazole-treated groups, respectively. The number of up- and down-regulated transcript were approximately equal at each timepoint, with the exception of the 3-day timepoint, at which only 26% of the transcripts exhibiting significant changes were upregulated. For the T3-treated groups, 1961 and 1680 transcripts were identified as differentially expressed for the 3-day and 1-week timepoints, respectively. Again, the numbers of up- and down-regulated genes were approximately equal in these arrays. Fifteen genes that sampled the full range of fold-changes from low (1.8-fold) to high (13.6-fold) were selected for validation by qRT-PCR. All 15 exhibited changes in expression by qRT-PCR (Table 1) that followed the same trend as the microarray data although, due to differences in the nature of the methods, their changes were generally greater in magnitude than was seen on the arrays (see Discussion).

The full set of genes whose expressions changed significantly is presented in Supporting Information Tables 1 and 2. For our discussion here, we concentrate on those that were upregulated, primarily with methimazole treatment, because we wanted to see whether this paradigm could be used to highlight specifically those genes associated with successful regeneration. Such genes would be expected to be upregulated under regeneration-permissive (methimazole-treated, post-injury) conditions and not under regeneration-inhibitory conditions (T3-treated, post-injury). There were 53, 162 and 133 transcripts upregulated at the 3-day, 1-week, and 3-week timepoints, respectively, in this category. Only the 72 that were either annotated in the *Xenopus* database or could be identified by BLAST search as prospective homologs to known genes in other systems are listed; ESTs and transcripts that have no known function or homolog from which a function could be inferred are not listed (Table 2).

The first five genes listed [suppressor of cytokine signaling 2 (SOCS2), XER81, neurotensin (NTS), MORC3 and RNA polymerase II subunit 5-mediating protein (RMP)] may be particularly relevant to successful regeneration. These genes were upregulated under regeneration-permissive conditions (methimazole) but down-regulated under inhibitory conditions (T3-treated). The next eight were those that increased in expression under regeneration-permissive conditions relative to inhibitory ones at more than one timepoint after transection, suggesting that they may be important for maintaining the axonal growth-active state. Three of these were transcription factors [myocyte enhancer factor 2C (MEF2C), FOS and teashirt zinc finger 3 (TSHZ3)]; the other five [axial protocadherin (AXPC), RAS protein activator-like 2 (RASAL2), HSPC150, TRIO, and a gene homologous to C2orf37] have putative roles in intracellular signaling or cell–cell communication. The remaining 59 transcripts are listed according to the timepoint when their expression increased. Collectively, these latter genes included seven transcription factors, fifteen membrane proteins, eleven intracellular signaling proteins, three cell–cell signaling proteins and four nuclear proteins involved with transcriptional regulation. An additional seventeen fell into other functional categories, and two additional genes were of unknown function.

We also looked at those genes upregulated after injury under regeneration-inhibitory conditions (T3-treated). We anticipated that there would be many more genes upregulated in this group than with methimazole treatment, as this group would include both those genes activated by TH and those activated by the injury; this was indeed the case. At 3 days and 1 week after transection, 880 and 758

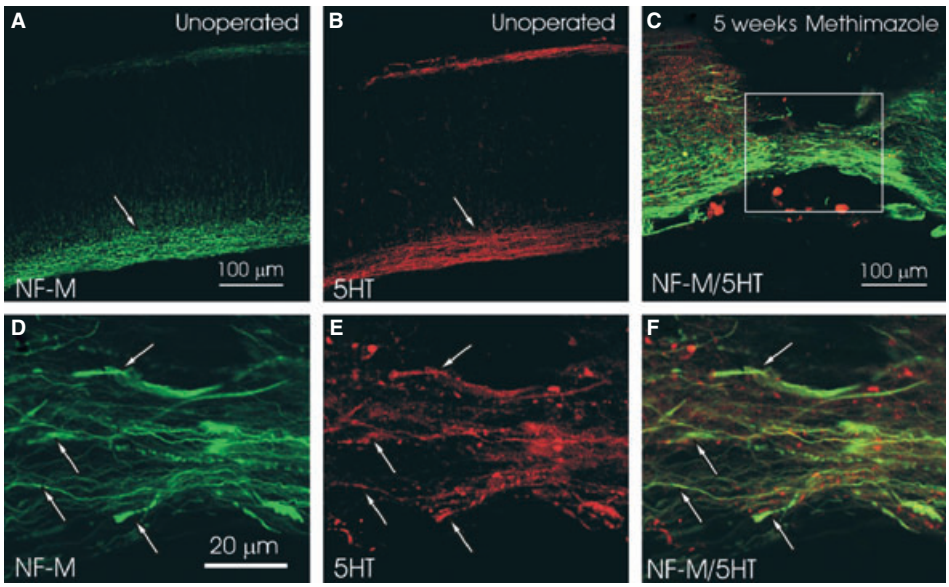

FIG. 4. Serotonergic axons crossing the lesion site in a methimazole-treated tadpole at 5 weeks. Parasagittal cryosections were immunostained for NF-M (green) to label axons, and for serotonin (red) to identify axons within the descending tracts originating from reticular and raphe nuclei (see text). (A and B) A low-power view [20 ×, 0.75 NA; one optical section – 1.3, 1.3, 2.1 μm (x, y, z)] of a parasagittal section through the spinal cord of an unoperated animal to illustrate the presence of serotonergic axons within the descending tract. NF-M (A, green) and serotonin (B, red) immunostraining are shown separately. (C) A low-power view [20 ×, 0.75 NA; one optical section – 0.9, 0.9, 2.1 μm (x, y, z)] of descending axons crossing the lesion site (boxed region). NF-M (green) and serotonin (red) immunostaining are superimposed. (D–F) View of the boxed region in C at higher magnification [63 ×, 1.4 NA; one optical section – 0.14, 0.14, 0.3 μm (x, y, z)], with NF-M (green) and serotonin (red) immunostaining viewed separately in D and E, respectively, and superimposed in F. Arrows point to examples of axons double-labeled for NF-M and serotonin. Dorsal is up, and rostral is to the left. Scale bar in A also applies to B, and that in D also applies to E and F.

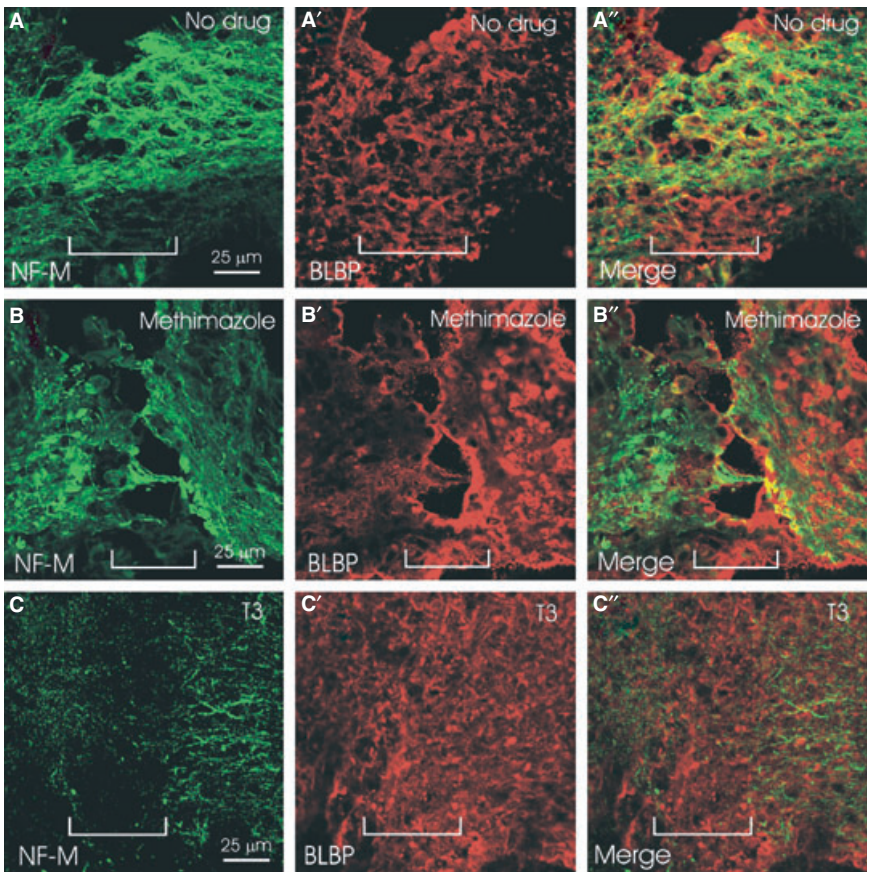

FIG. 5. Regenerating axons follow radial glia across the lesion site in untreated (A–A″) and methimazole-treated (B–B″), but not in T3-treated (C–C″) tadpoles. Axons and radial glia are labeled by immunostaining for NF-M (green, A–C) and BLBP (red, A′–C′), respectively. Channels are shown separately in A–C and A′–C′ and are merged in A″–C″. Each image represents a single optical section [A, B – 20 ×, 0.75 NA; 0.3, 0.3, 2.1 μM (x, y, z). C – 20 ×, 0⁄75 NA; 0.5, 0.5, 2.1 μM (x, y, z)] of a parasagittal anatomical section; rostral is to the left. The lesion site is indicated by a horizontal bracket.

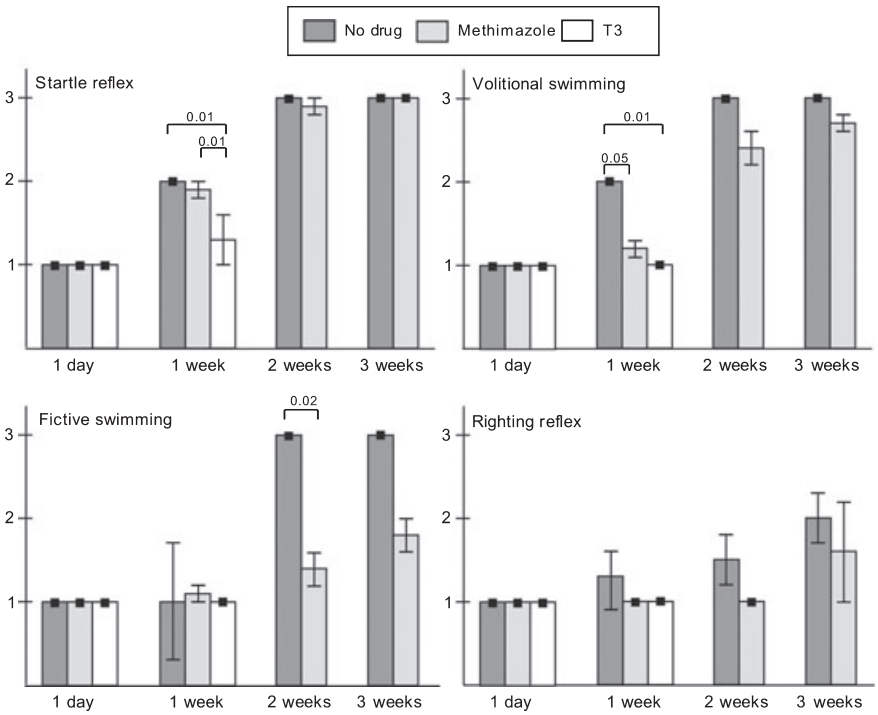

FIG. 6. Influence of TH on the functional recovery of spinal-mediated behaviors. *Xenopus laevis* tadpoles (NF stage 51–53) received complete spinal cord transection and were allowed to recover with no drug treatment (n = 3), 1 mM methimazole treatment (n = 14) or treatment with 5 nM T3 (n = 18). At 1 day and 1 week (no drug, methimazole, T3), and at 2 and 3 weeks (no drug, methimazole), behaviors were visually scored for each animal as being either absent (1), present but abnormal (2), or qualitatively normal (3). These scores were then averaged over each group; bars are SEM. Treatment regimens and behaviors are as described in the text. Downward-facing brackets indicate statistically significant (two-sided Wilcoxon–Mann–Whitney U-test) pairwise comparisons within each time point.

transcripts, respectively, (including ESTs) were upregulated by our filtering criteria. Because of their large number, we present here (Table 3) only a subset of these genes that we think will be of particular interest to the readership. The complete list of annotated and deduced homolog genes is presented in Supporting Information. Among those listed are known TH response genes (e.g. Lzip8, Bteb1, Dio3, Collagenase 3, Gene 16, NFIX2), whose presence served to validate the drug treatment paradigm. Still others could potentially play a role in affecting axon regeneration, either through their known involvement in established relevant mechanisms or because they represent factors previously identified as being involved in transcription, tissue remodeling, chromatin modification or signal transduction (see Discussion). Table 4 presents those genes whose expressions increased with both methimazole and T3 treatment after spinal cord transection. Their increased expression under both treatments suggests that they are related to either a generalized injury response or to stress.

Expression of GAP-43, peripherin and NF-M in the no-injury condition

Three genes often associated with axonal growth in other systems were noticeably absent from the transcripts that were upregulated after transection under regeneration permissive conditions – GAP-43 (Skene *et al.*, 1986), the middle neurofilament protein (Jacobs *et al.*, 1997; Gervasi *et al.*, 2003) and peripherin (also known as plasticin in fish) (Asch *et al.*, 1998; Gervasi *et al.*, 2003). In the anamniote visual system, these genes generally exhibit a stereotypical temporal expression pattern after optic nerve injury that correlates with regenerative success. GAP-43 and peripherin are upregulated soon after injury and return to pre-injury levels when regeneration is complete. NF-M is initially downregulated, then rises to supranormal levels during the peak period of axonal regrowth, and eventually returns to normal levels of expression when regeneration is complete. These same genes are also usually upregulated during developmental axonal outgrowth. Although their expressions fluctuated after spinal cord transection, the changes in expression seen for these genes failed to meet our criteria for significance for any of the operated groups (Fig. 7).

We considered two possible explanations for this result: (i) regenerative changes in the reticular and raphe neurons were too small to be detected biochemically from whole hindbrain; and (ii) larval tadpoles express these genes at a level consistent with hindbrain motor neurons being in a growth-primed state, allowing them to maintain the CNS plasticity required during metamorphosis. To determine how the expression of these genes changed in hindbrain neurons that regenerate, we performed *in situ* hybridization on spinal cord-transected tadpoles and age-matched controls, both without drug treatment. These experiments revealed that all three genes were already expressed abundantly in raphe and reticular neurons of unoperated tadpoles and confirmed that their expressions did not change appreciably in these neurons with injury. Thus, these data favored the second possible interpretation.

Discussion

Our data indicated that tadpoles could regenerate axons across a spinal cord lesion and functionally recover when metamorphosis was pharmacologically arrested. Conversely, pharmacologically accelerating metamorphosis led to the failure of axons to regrow and to paralysis. Thus, prometamorphosis is not a requirement for successful recovery from spinal cord injury, whereas prematurely accelerating metamorphosis is sufficient to inhibit it.

TABLE 1. Microarray validation

Gene name	Primers	Fold change	
		Microarray	qRT-PCR
SOCS2	(F) GTGGCTGGTGAA GCCACTAT (R) TGTTCCAATGCTTAACTGATG	1.9	3.5
Neurotensin	(F) GAGGAACCAGAAGAAACTGG (R) ACTGTTTGGGCTGTTAGGTT	2.0	7.4
XER81	(F) GCAAGAAAATCTTCCTCCTACA (R) CAAGGAGTGCTTGCTGTATC	1.8	3.4
RPB5	(F) TCCCAAGAAGTTCGAGAATC (R) TCAACTGTGTGCAGAAAATG	1.8	2.8
XPcl-2	(F) AGCATGGAGCAGAGTAATCA (R) TGAGGCATAGGTCCCATAGT	2.8	6.4
TRIO	(F) AGTTGATCCTTCCCAGCTAA (R) TTGCAAGCATCTCCTGTAGT	2.0	4.8
FGF8b	(F) AATTTCCTGAACTCCTTTGC (R) CACAACATTT TTGCTCATCA	2.0	9.3
Tsh3	(F) CACAAACTAAATCCCCTTCTG (R) GTGATCCTCGGGTGATTT	2.3	3.2
Bteb-1a	(F) TTTCTCGTTCCGATGAGTTA (R) TCAGGTGAATGATGAATTGG	13	4181*
Fizzy1	(F) ACACTGCTCGAGTGCTTAAT (R) AGTTTGTTCATCGGATGCTT	2.5	17
Activin Beta b	(F) TCACATACACTGGACAGGAA (R) GTGGACTCAGTGCAAAACAT	4.4	42
Insulin induced gene-1	(F) GTGGGAAGGGAAATCATGT (R) ATCCACTTTTTGGGATTCAG	1.9	24
MCpGBP	(F) TTTCTGTGGAGAAATACCTGTT (R) GCAATTAGTAGCTTGAAAAAGTTC	2.7	77
ZNF395	(F) AATCT TCGCT ACACG GAAGT (R) TTGAGGAGGTTAAAATGTACG	−12	−2.4
C3H-1	(F) TGTGTCCTACCTCACAGTTACA (R) ACACATTAGAAGAAGCACACTTT	−2.3	−1.5

Genes used to validate microarray data as being differentially expressed. Fifteen genes identified by microarray analysis as having a change in expression ≥ 1.8-fold were validated using qRT-PCR. Genes were selected to represent both methimazole- and T3-treated groups across a broad range of expression values. An asterisk (*) is used to denote extremely large changes in expression due to the absence of detectable expression in control vs. experimental samples.

Nearly all vertebrates exhibit at least some ability to regenerate spinal cord axons during embryonic development. Recovery in these developing animals may involve both axon regeneration and the *de novo* establishment of parallel neural pathways (Ten Donkelaar, 2000). Sequential application of two different dyes that are taken up specifically by cut axons provides direct evidence for regeneration (Zhang & McClellan, 1999). Indeed, such an approach has demonstrated in *Xenopus* tadpoles that raphe and reticular axons regenerate reliably (Gibbs & Szaro, 2006). This double labeling study validated an earlier approach utilizing immunostaining for serotonin as evidence for regeneration (Beattie *et al.*, 1990; Ten Donkelaar, 2000). The basis for this second approach is that serotonergic axons of the ventral tract principally originate from reticular and raphe neurons. Because the serotonergic neurons in these nuclei are born well before the time of transection, any such axons appearing within the lesion site are unlikely to represent parallel projections arising *de novo* (van Mier & Ten Donkelaar, 1984). The use of double labeling was precluded in the present study because methimazole and T3 treatment resulted in animals that were less robust, and survival periods were not long enough to allow for the second round of labeling. Given the validity of using serotonin immunostaining as an indication of regeneration in untreated animals, along with the observation that arresting metamorphosis also inhibits the proliferation of neurons that might potentially contribute to *de novo* pathways (Marsh-Armstrong *et al.*, 2004), we felt that the presence of serotonergic axons crossing the lesion site in methimazole-treated tadpoles provides strong evidence for axon regeneration.

Our findings also indicate that although prometamorphosis is not necessary for recovery it may nonetheless help promote it. Tadpoles undergoing no drug treatment exhibited more rapid and complete reconstitution of the injured spinal cord, more NF-M-positive axons crossing the lesion, and more rapid functional recovery than did those treated with methimazole. Untreated tadpoles develop normally and thus synthesize low levels of TH during the first week after surgery, which might facilitate recovery. The wide ranging effects of TH suggest a number of possible mechanisms for this. As TH increases brain metabolism (Denver *et al.*, 1997), some of its effects could be due simply to increased metabolic rate. TH also promotes neuro- and gliogenesis (Kollros, 1981; Marsh-Armstrong *et al.*, 2004; Denver, 2008), both of which could accelerate recovery. Increased gliogenesis in particular could have contributed to the improved wound healing and tissue remodeling that was seen in untreated tadpole, as well as the more uniform BLBP staining that filled the lesion site of T3-treated tadpoles. TH is also known to affect the expression of extracellular matrix proteins such as fibronectin and integrins (Brown *et al.*, 1996) as well as tissue remodeling enzymes such as matrix metalloproteinases (Shi & Brown, 1993; Wang & Brown, 1993; Damjanovski *et al.*, 1999). Indeed, collagenase 3, a matrix metallopoteinase (MMP 13), was upregulated on T3 arrays but absent from methimazole arrays.

Although T3-treated tadpoles exhibited many similarities with juveniles in their response to spinal cord transection, they differed in some respects, such as in the appearance of the wound at 1 week. Typically, TH levels rise from stages 54 to 61, then decline to adult

TABLE 2. Genes upregulated in methimazole-treated spinal cord-transected tadpole

			M			T3	
Unigene	Category	Gene name	3d	1w	3w	3d	1w
Xl.50377	CP/ICS	SOCS2	1.9		1.9		−1.8
Xl.47572	CCS/L	Neurotensin/neuromedin N		2.0		−3.0	−2.5
Xl.33162	NP	HP: MORC3		1.9		−2.0	−2.3
Xl.76067	TF	XER81			1.8	−2.2	
Xl.47364	NP/Transc	Similar to RPB5-mediating protein			1.8		−1.8
Xl.47612	TF	MEF2C	2.3	2.9	2.5		
Xl.63092	CCS/MR	Axial protocadherin	1.8	2.2			
Xl.10283	TF	V-fos	1.8		2.0		
Xl.9022	TF	Tsh3	2.3	2.4	2.1		
Xl.50386	ICS	HP: RAS protein activator like 2		2.2	1.8		
Xl.12282	ICS/UB	HSPC150	1.8	1.9			
Xl.57698	Uncharacterized	HP: C20rf37 homolog		2.0	1.9		
Xl.50094	ICS	HP: TRIO	2.1	2.0			
Xl.30	TF	v-kit Hardy-Zuckerman	2.7				
Xl.14315	NP	Predicted: JAR1D2	2.6				
Xl.77217	Uncharacterized	HP: C10rf174 homolog	2.4				
Xl.53666	MP	Similar to CCDC51	2.3				
Xl.57336	ICS	HP: Casein kinase 1, γ3, 2	2.1				
Xl.21708	rRNAP	HP: Tsr2	2.0				
Xl.12384	ICS/UB	Similar to: Vpr-binding protein	2.0				
Xl.29378	ER	PDI A6	2.0				
Xl.51787	MP	HP: SLC19A2	1.9				
Xl.4290	MP/ICS	HP: PAF	1.9				
Xl.968	ICS/UB	BTRC-a	1.8				
Xl.58749	MP/IF	HP: MHC class II beta-chain	1.8				
Xl.34346	TF	Predicted: Homeo box D4		5.7			
Xl.52966	TF	Polycomblike 2		2.8			
Xl.21606	MP/IF	T-cell receptor alpha		2.6			
Xl.78192	MP/Mito	HP: SMCR7L		2.4			
Xl.75878	ICS	HP: NEDD4 binding protein 2		2.4			
Xl.14717	MP	HP: Transmembrane protein 30A		2.3			
Xl.2761	NP/Transc	HP: NCOR1		2.3			
Xl.47451	MP/Mito	Outer membrane protein 25		2.1			
Xl.57242	ICP/Met	HP: ATAD2B		2.0			
Xl.20011	CCS/L	FGF-8b		2.0			
Xl.50196	NP	HP: SH3BGRL2		1.8			
Xl.48897	ICS/UB	MGC85526 protein: ASB5		1.8			
Xl.47315	MP/CA	MGC80200 protein: NCAM2 (Nr-Cam)		1.8			
Xl.66298	ER	ER-resident kinase PERK		1.8			
Xl.21608	MP/ICS	Cannabinoid receptor 1/CB1		1.8			
Xl.59866	MP/ICS	TMEFF2		1.8			
Xl.71886	ICS	Predicted: similar to CTNNAL1			5.3		
Xl.688	TF	Thyroid transcription factor 1			3.6		
Xl.57018	CP	HP: PHLDA2			3.0		
Xl.29880	ICS	HP: centaurin, alpha 1			2.6		
Xl.21419	RNA met	HP: SRRM1			2.6		
Xl.564	MP/SV	Synapsin IIa			2.4		
Xl.65736	TF	C-Fos a			2.3		
Xl.50787	Mito	PDP2			2.3		
Xl.47578	ICS	HP: DOCK9			2.2		
Xl.25798	Mito	PCCA			2.1		
Xl.48881	Uncharacterized	Predicted: similar to FAM135B			2.1		
Xl.9988	IC/Ptase	HP: PRSS16			2.0		
Xl.52035	ICS	Mdm4 protein			2.0		
Xl.68850	RNABP	HP: RBM 42			1.9		
Xl.21633	MP	GRIK2			1.9		
Xl.2599	RNAmet	SF3B1			1.9		
Xl.48462	ICS	HP: LRRK2			1.9		
Xl.41591	TF	HP: HDGF			1.9		
Xl.637	TF	EGR 1			1.9		
Xl.23598	CCS/L	Tgfb2-A			1.9		
Xl.23524	ICP	HSD17B6			1.9		
Xl.34486	MP/ICS	HP: PLEKHB2			1.9		
Xl.13872	CCS	Slit homolog 1			1.9		
Xl.54918	ICP/Ptase	HP: similar to DPP8			1.8		
Xl.56564	CP/Met	HP: PYGM			1.8		
Xl.55591	CP/Cyskl	HP: similar to radixin			1.8		
Xl.23550	CP/Motor	HP: Kif19			1.8		

TABLE 2. Continued.

			M			T3	
Unigene	Category	Gene name	3d	1w	3w	3d	1w
Xl.47139	NP/Transc	HP SMARCC2			1.8		
Xl.14482	NP/Transc	Wilms tumor 1 interacting protein			1.8		
Xl.55111	NP/Transc	HP: TRIP 11			1.8		
Xl.29836	MP/ICS	Proprotein convertase 4			1.8		

Genes upregulated in hindbrain following spinal cord transection under regeneration-permissive conditions (methimazole-treated). Hindbrains of methimazole-treated tadpoles were harvested and analyzed by arrays at 3 days (3d), 1 week (1w) and 3 weeks (3w) following complete spinal cord transection. The fold-change relative to methimazole-treated, unoperated control is listed under each relevant timepoint. Fold increases and decreases are positive and negative, respectively. Unlisted values indicate either a < 1.8-fold change or one that was statistically nonsignificant. The first five were upregulated with methimazole (M) and downregulated with T3 treatment. The next eight were upregulated with methimazole at all timepoints. The remaining were upregulated at only the indicated timepoint. Each gene is designated by its UniGene ID (left column). Gene names and function were assigned as described in Materials and methods. Abbreviations: CA, cell adhesion; CCS, cell-cell signaling molecule; CP, cytoplasmic protein; cyskl, cytoskeletal protein; ER, endoplasmic reticular protein; ICP, intracellular protein; ICS, intracellular signaling molecule; IF, immune function; L, receptor ligand; Met, metabolism; Mito, mitochondrial protein; motor, motor protein; MP, membrane protein; MR, membrane receptor; NP, nuclear protein; RNA BP, RNA binding protein; RNA met, RNA metabolism; rRNAP, ribosomal RNA protein; SV, synaptic vesicle component; TF, transcription factor; Transc, gene involved in transcription; UB, involved in ubiquitination; Uncharacterized, function uncharacterized.

levels (Leloup and Buscaglia, 1977; Simon *et al.*, 2002). The tight temporal control of TH production, together with variations in TH responsiveness among individual tissues, ensures the correct developmental expression of genes required for metamorphosis (Etkin & Gilbert, 1968; Dodd & Dodd, 1976; Shi, 2000). Exposure to 5 nM T3 accelerates this process, but not instantaneously. For example, it takes 2–3 days of exposing premetamorphic tadpoles to 5 nM T3 for the hormones prolactin and somatostatin, whose syntheses are controlled by TH, to reach the levels typical of metamorphic climax (Buckbinder & Brown, 1993). Such a delay in the time needed for T3 to elicit its full effects could therefore have contributed to differences in wound healing seen between T3-treated tadpoles and untreated juveniles. Molecular data from the T3 arrays support this possibility. Silencing Mediator for Retinoid and Thyroid receptors (SMRT) is part of the transcriptional repressor complex that is recruited by TH receptors (and other nuclear hormone receptors) and relieved by TH binding (Horlein *et al.*, 1995). Its expression should be suppressed by TH, as was indeed the case at 1 week. However, at 3 days it was still present in T3-treated animals, suggesting that TH levels in hindbrain were still insufficient to reduce its expression. These differences between T3-treated tadpoles and untreated juveniles notwithstanding, T3 treatment clearly altered the injury response significantly by transforming regeneration-permissive larval conditions into inhibitory ones. These observations thus strengthen the causal connection between the cascade of events triggered by rising levels of TH, which drives the transformation from the larval to the adult form, and the developmental loss of regenerative capacity in spinal cord.

Thus, it can be argued that in *Xenopus* it is the maintenance of larval features that is needed for spinal cord axon regeneration. The ability of amniotes to recover from spinal cord injury is also lost at some point during development, suggesting that certain larval features may also be important for promoting recovery among the so-called 'higher' vertebrates. One such larval feature is the presence of radial glia which, in amniotes, are characteristically more prominent in the developing than in the adult CNS. Radial glia, which express BLBP (Feng *et al.*, 1994), form scaffolds for migrating neurons and guide growing axons during mammalian development (Norris & Kalil, 1991). In mammals, BLBP-expressing embryonic radial glia promote spinal cord axon regeneration as well as decreased expression of growth-inhibitory factors (Hasegawa *et al.*, 2005); in turtle, they appear to guide regrowing axons in transected spinal cord, which exhibits axonal regrowth (Rehermann *et al.*, 2009). Consistent with these observations in amniotes, axons crossing the lesion site in untreated and in methimazole-treated tadpoles frequently co-localized with BLBP-positive radial glial fibers; however, with T3 treatment, BLBP was abundantly expressed within the lesion site but did not co-localize with axons (NF-M). These results suggest that T3 treatment impaired the capacity of axons to regenerate and of radial glia to facilitate this regeneration without impairing the ability of radial glia to invade the lesion site during wound healing.

Based on our results, we also concluded that the developmental loss of axonal regenerative capacity in *Xenopus* spinal cord occurred as a direct consequence of the developmental events triggered by rising levels of TH. Our data are consistent with a model wherein the low levels of TH present early in prometamophosis help to promote wound healing through increased gliogenesis but later lead to the inability of hindbrain neurons to activate the axonal growth program as TH levels rise during metamorphic climax. Rising TH levels also correlate with the loss of forelimb regenerative potential in *Xenopus* tadpoles, with complete loss occurring at metamorphic climax (Dent, 1962). However, rising levels of TH probably also work in concert with cell type-specific levels of sensitivity and responsiveness to TH in determining regenerative capacity, as retinal ganglion cells in *Xenopus* maintain their capacity to regenerate an axon throughout life (Taylor *et al.*, 1989). In anuran CNS development, TH stimulates extensive tissue remodeling through neuro- and gliogenesis, apoptosis, and increased myelination, all directed toward accommodating the adult form (Weiss & Rosetti, 1951; Kollros, 1981; Will, 1986; Ten Donkelaar, 2000; Marsh-Armstrong *et al.*, 2004). Brain development in amniotes during late fetal and post natal stages also critically depends on TH (Howdeshell, 2002). Interestingly, the loss of regenerative capacity of spinal cord axons in both chick and rodent occurs after the onset of TH exposure. Chicks begin producing TH endogenously at E10 and lose spinal cord axon regenerative capacity at E13 (Hasan *et al.*, 1993; Muchow *et al.*, 2005); rats become exposed to maternal TH at E9 leading to a steady rise in circulating TH levels, and they lose regenerative capacity by E15 (Saunders *et al.*, 1992; Howdeshell, 2002). Thus, the negative effects of high levels of TH on regeneration of spinal cord axons seen here in *Xenopus* could also have implications for the loss of regenerative capacity in amniotes.

TABLE 3. Genes upregulated in T3-treated spinal cord-transected tadpole

Unigene	Category	Gene name	T3, 3d	T3, 1w
Xl.453	TF	Leucine zipper gene 8	27.8	16.4
Xl.353	ECP	Collagenase-3	15.8	18.6
Xl.347	TF	Bteb 1a (KLF9)	13.6	8.5
Xl.13228	NP	Centromere protein N	9.7	
Xl.54050	CCS/L	HP: BMP 6	8.4	5.2
Xl.8196	MP	SLC15A2	6.4	2.0
Xl.862	MP	Deiodinase, iodothyronine, type III	6.3	3.4
Xl.3204	ICP/ER	Heavy-chain binding protein BiP	5.0	2.3
Xl.1090	SP	Activin Beta b	4.4	4.1
Xl.25391	NP	HP: Apoptosis-enhancing nuclease	4.0	
Xl.2213	CP/ICS	HP: SOCS 3	4.0	
Xl.21563	MP/Mito	TGM2	4.0	4.5
Xl.55631	SP	HP: TIMP 3	3.9	2.0
Xl.77410	NP	HP: IFRD1	3.7	
Xl.73282	MP/Golgi	HP: RAB36	3.5	2.9
Xl.16548	CCS	HP: Netrin 1	3.4	2.5
Xl.70833	CP	Methionine-tRNA synthetase	3.2	
Xl.4203	ICP	ABCF2	3.0	2.0
Xl.57034	TF	Nuclear factor I-C1	3.0	
Xl.48217	CP	Heat shock protein 105	2.9	2.2
Xl.481	TF	Zinc finger protein Gli2	2.9	
Xl.55978	Uncharacterized	HP: Similar to ZNF 711	2.8	
Xl.8364	NP	MBD3	2.7	2.0
Xl.33920	NP	MGC84310: CHMP2B	2.7	2.6
Xl.620	SP	Wnt inhibitor Frzb3-like	2.6	2.3
Xl.357	ICP	Gene 16	2.6	
Xl.3026	CP/ICS	Adenylate kinase 7	2.6	2.2
Xl.4938	NP	Fizzy1 (CDC20)	2.5	
Xl.20608	MP	Transmembrane protein 177	2.5	
Xl.693	CP/ICS	CaM kinase II gamma	2.4	2.7
Xl.1099	MP/ICS	Receptor protein tyrosine phosphatase beta.11	2.4	2.7
Xl.3540	MP/ICS	p75-like transmembrane protein fullback	2.3	
Xl.1396	TF	Forkhead box protein	2.2	2.2
Xl.14056	CP/ICS	RAN GTPase activating protein 1	2.2	
Xl.7678	NP/Transc	HP: REST corepressor 2	2.1	1.9
Xl.25554	CP/ICS	MGC80232 SOCS1a	2.1	
Xl.23295	NP	Protein arginine methyltransferase 1	2.0	
Xl.60871	CP	HP: HSPA (Heat shock 70 kDa) binding protein	2.0	
Xl.25554	CP/ICS	HP: SOCS1	2.0	
Xl.48463	MP/ER	Insulin induced gene 1	1.9	
Xl.26031	TF	Activating transcription factor 5	1.9	
Xl.973	TF	Homeobox protein Xgbx-2		2.9
Xl.50412	CP	HP: chondroitin 4 sulfotransferase 11		2.3
Xl.21537	MP/ICS	Receptor protein tyrosine phosphatase Rho precursor		2.2
Xl.21440	MP	Metalloprtease/disintegrin xMDC11.1		2.2
Xl.21565	MP/ICS	Neural cell adhesion molecule L1		2.2
Xl.54777	CP/ICS	Intersectin		2.1
Xl.741	CP/ICS	Smad8C protein		2.0
Xl.166	MP	ADAM 13		2.0
Xl.1096	TF	NFI-X2 transcription factor		2.0
Xl.48321	MP/ICS	FGF receptor-like protein		2.0
Xl.41403	CP/UB	F-box protein 11		2.0
Xl.21607	MP/ICS	Thyrotropin-releasing hormone receptor 3		2.0
Xl.78076	ICS	Nerve injury gene 283		1.9
Xl.23456	CP	Neurochondrin		1.9
Xl.79277	CP/ICS	Hypothetical protein: RhoGap68f		1.8
Xl.3801	ICS	Neuronal nitric oxide synthase 1		1.8
Xl.58616	TF	Zinc finger, MYND domain-containing 10		1.8
Xl.76580	NP	HP: Suppressor of zeste 12 homolog		1.8

Selective genes upregulated in hindbrain after spinal cord transection under regeneration inhibitory conditions (T3-treated). Abbreviations and other details are as in Table 2. See Supporting Information for the full listing.

Expression profiling

Gene expression profiling on microarrays provided direct evidence for intrinsic changes in hindbrain neurons during a successful regenerative response to spinal cord injury. Treatment of tadpoles with methimazole permitted for the first time the analysis of changes in gene expression during regeneration in the absence of background changes resulting from ongoing development. Structural genes that typically increase with axon outgrowth in other systems [e.g. GAP43 (Jacobson *et al.*, 1986; Skene *et al.*, 1986) and peripherin (Gervasi *et al.*, 2003)] were found already abundantly expressed in hindbrain of normally developing tadpole at these stages, by both microarray and *in situ*

TABLE 4. Genes upregulated in methimazole- and T3-treated spinal cord-transected tadpole

			M			T3	
Unigene	Category	Gene Name	3d	1w	3w	3d	1w
Xl.74164	ICP/Mito	Similar to: CDKN2D	4.3				5.4
LOC733250	MP	HP: Glycoprotein NMB	2.7	2.0	2.5		3.1
MGC132043	CCS/L	HP: Tachykinin 1 isoform 1	2.0				1.8
Xl.21031	MP/ICS	PTPRD	2.0	2.1	2.0	2.2	2.3
Xl.28411	NP	HP: NCOR2	3.3	3.5	3.6	3.7	
Xl.48433	CP	HP: Hook3	3.0	2.9		2.2	
Xl.826	TF	Myc-A		1.8	1.9	2.0	
Xl.9047	TF	Homeobox C5		5.5			6.8
Xl.8804	TF	HP: CBX 6		2.2			2.0
Xl.82524	ICP	HP: Cathepsin S		3.7			3.5
Xl.18619	ICP	HP: Similar to LIPE			1.8		2.0
Xl.77747	NP/Transc	HP: Prdm2 protein			2.4		2.9
Xl.32812	CP/Syn	Rabphilin 3A homolog			2.0		1.8
Xl.6687	CP	Similar to: BLBP		2.8		6.0	2.4
Xl.12862	MP/Apop	MFGE8		1.8		1.9	3.2
Xl.60293	NP/Transc	HP: TR beta B2		2.2		3.6	2.2
Xl.1109	MP	Gap Junction α1, 43 kDa		1.8			3.4
Xl.24560	Sec	HP: α-2-HS-glycoprotein		2.1		2.0	2.0
Xl.5377	MP	Similar to: P4HB		1.8		2.6	2.0
Xl.82105	MP	HP: Similar to CYP26C1		3.2	3.0	3.2	7.1

Genes upregulated in both methimazole- and T3-treated tadpoles following complete spinal cord transection. Abbreviations and other details are as in Table 2.

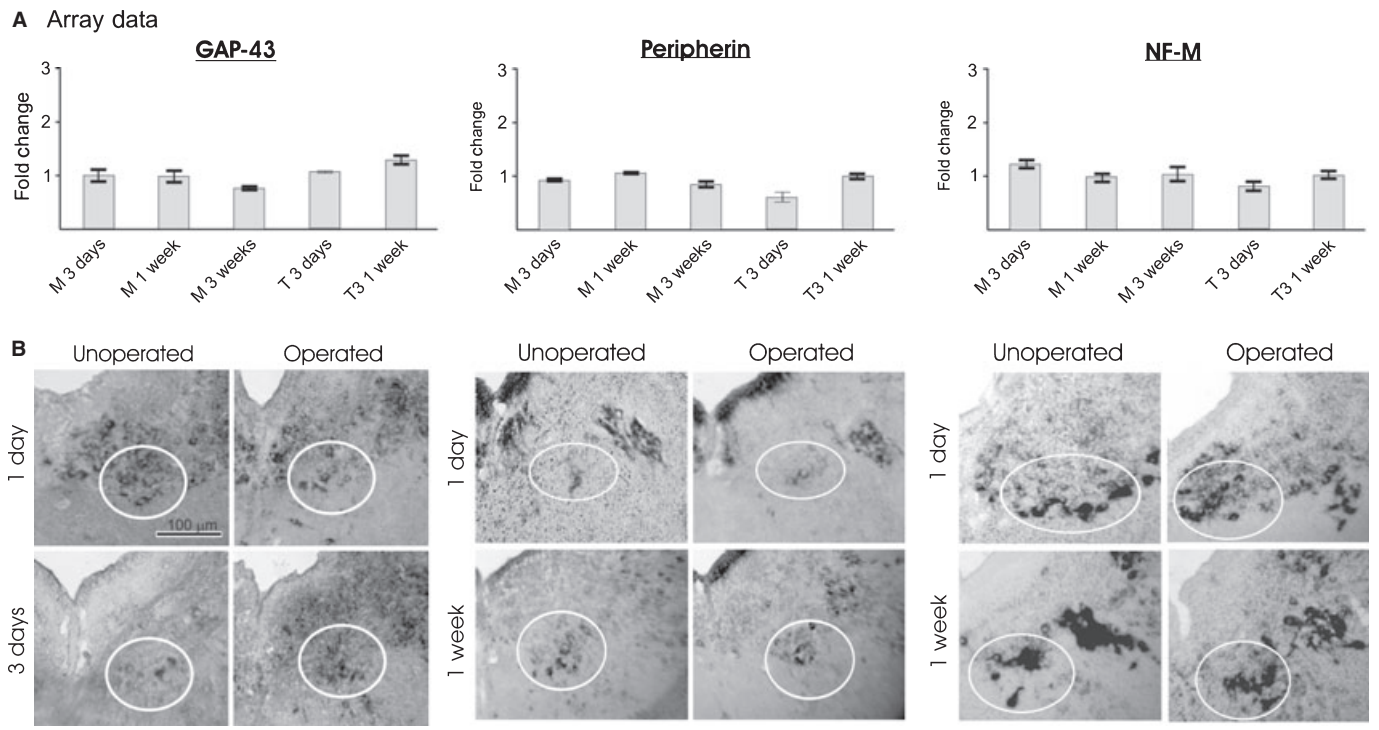

FIG. 7. GAP-43, peripherin and NF-M expression in hindbrain after spinal cord transection. (A) Microarray data indicating that no significant change in expression of these mRNAs took place. Abbreviations – M, methimazole-treated; T3, T3-treated; 3D, 3 days; 1W, 1 week; and 3W, 3 weeks after spinal cord transection. (B) *In situ* hybridization with digoxigenin-labeled cRNA probes to GAP-43, peripherin and NF-M in transverse sections of hindbrain without drug treatment, at the indicated times after spinal cord transection and in age-matched uninjured controls. Hybridized probes were visualized by immunohistochemistry with an alkaline phosphatase-labeled antidigoxigenin antibody. Expression in reticular neurons (circle), which are known to regenerate an axon under these conditions, is equivalent for all three genes between operated and unoperated tadpoles, suggesting these neurons were already in a 'growth-primed' state prior to the injury. The calibration bar in the GAP-43, unoperated, 1-day panel applies to all panels.

hybridization. These data are consistent with the idea that the larval state of tadpoles is already conducive to regeneration and, as such, elevated expression of these structural genes need not be induced *de novo* with injury. Nevertheless, spinal cord transection was sufficient to induce specific sets of new genes and inhibit still others in the methimazole-treated maintained larval state.

Five genes in particular increased after injury in the methimazole-treated (regeneration-permissive) condition and were selectively

downregulated in the T3-treated (regeneration-inhibitory) condition – SOCS2, XER81, MORC3, NTS and RMP. Interestingly, four of these five have known functions consistent with promoting neuronal development, survival and neurite outgrowth: (i) SOCS2 promotes neurite outgrowth in cortical neurons and in PC12 cells, where its expression inhibits RhoA and activates Rac1 through the SOCS2-mediated phosphorylation of epidermal growth factor receptor (EGFR) (Goldshmit *et al.*, 2004); (ii) XER81 is a transcription factor expressed by mammalian corticospinal neurons that is required for establishing correct sensory–motor connectivity in developing spinal cord (Arber *et al.*, 2000; Hevner *et al.*, 2003); (iii) Morc3 is a nuclear protein shown to activate p53 (Takahashi *et al.*, 2007), which is necessary for neurite outgrowth in cultured neurons and for facial nerve regeneration (Di Giovanni *et al.*, 2006); (iv) NTS is a neuropeptide that antagonizes the binding of proNGF to the sortilin receptor (Mazella *et al.*, 1998; Nykjaer *et al.*, 2004) which in the CNS is a co-receptor with p75 receptor for proNGF; proNGF binding to this receptor complex promotes cell death. Thus, increased expression of NTS could play a potent role in neuroprotection; and (v) The fifth gene in this group, RMP, although not previously associated with neurite outgrowth and neuroprotection, is a transcriptional repressor that works in combination with DNA methyltransferase 1 (Dmap1; Delgermaa *et al.*, 2004). It may therefore be involved in regulating downstream genes important for regeneration. The majority of the remaining genes that were upregulated with methimazole and not with T3 treatment have known functions in transcription and in cell signaling as opposed to being purely structural genes. This entire list presents a set of intriguing candidates for further studies aimed at dissecting the functions and regulatory pathways of these genes during injury.

With few exceptions, the magnitude of changes on the arrays was always smaller than that seen with validation by qRT-PCR. This phenomenon is common with array studies and thus the changes seen on microarrays should not be taken as quantitative measures of gene expression. Such measurements, particularly in a tissue as complex as hindbrain, are best done by qRT-PCR on samples recovered by laser-capture microdissection from the regenerating neurons themselves, a technically difficult method that goes beyond the current study. It should be noted that microarray studies have found changes as low as 1.5-fold to be biologically significant (Das *et al.*, 2009; Paulsen *et al.*, 2009), and thus our cutoff of 1.8-fold can be considered conservative.

T3 arrays were performed primarily to aid in the interpretation of the methimazole arrays. For example, the increased expression of many known TH-responsive genes on the arrays helped serve to validate the T3 treatment paradigm [e.g. Leucine zipper gene 8, Gene 16 and collagenase 3 (Brown *et al.*, 1996), Bteb (Denver *et al.*, 1997), Dio III (St.Germain *et al.*, 1994) and Nfi-x2 (Buchholz *et al.*, 2007)]. These genes were among those with the most robust responses. Next, we expected that genes associated more with injury and stress than with axon regeneration would be upregulated in both. Indeed, the known function of several such genes is consistent with this prediction. Tachykinin1 is a neuropeptide that is cleaved to produce other neuropeptides, including substance P, which is an important component of the response to pain and inflammation during CNS injury (Knerlich-Lukoschus *et al.*, 2008). Cathepsin S is a protease involved with antigen presentation in the microglial-mediated immune response (Nakanishi, 2003). AHSG is activated in multiple tissues, including brain, in response to chemically induced injury (Yoshida *et al.*, 1999). P4HB is a chaperone that is upregulated as a stress response gene; PTPRD (Johnson *et al.*, 2001) and L1 (Becker *et al.*, 1998) expression may represent an attempt by the damaged nervous system to initiate axon outgrowth. Also, BLBP was upregulated with both methimazole and T3 treatment, consistent with a response by radial glia in both groups.

In addition to these sets of genes on T3 arrays was an interesting set that, based on its members' known functions, could play a role in transforming the regeneration-permissive larval CNS into an inhibitory environment. For example, the expression of both SOCS1 and SOCS3 increased on T3 arrays. Both SOCS1 and SOCS3 inhibit cytokine signaling, and their expression negatively regulates STAT3. The inhibitory effects of SOCS1 and SOCS3 are directly counteracted by SOCS2 (Piessevaux *et al.*, 2006), whose expression increased under regeneration-permissive (methimazole) and decreased under regeneration-inhibitory (T3) conditions. Genes whose increased expression on T3 arrays is consistent with known inhibition of recovery from spinal cord injury include two additional genes: (i) *fullback*, which is closely related to p75 and has been implicated in dimerizing with other receptors to transmit growth inhibitory signals leading to axonal growth inhibition (Hutson & Bothwell, 2001); and (ii) ARHGAP1, a GTPase activator protein that inactivates the Rho family members Rho, Rac and Cdc42. ARHGAP1 has preference for Cdc42, which has been shown to promote neurite outgrowth (Lancaster *et al.*, 1994). Regardless of whether the genes that are upregulated with T3 treatment are directly involved in the inhibition of recovery from spinal cord injury or represent changes involved in the transition from larval to juvenile forms, their sheer number argues that the loss of regenerative capacity involves a change in developmental state evoked in hindbrain by TH. It remains to be seen whether similar changes take place at the injury site itself.

Taken together, these findings are consistent with TH being the principal activator of a cascade of developmental events that leads directly to the loss of the larval state and its attendant ability to execute the axonal growth program needed for axonal regeneration and functional recovery. Array studies indicated that both the response to injury and the loss of regenerative capacity necessarily involves multiple genes. Future studies aimed at characterizing the functions of these genes, along with their expression control mechanisms, could eventually lead to improved functional outcome from spinal cord injury in mammals.

Supporting Information

Additional supporting information may be found in the online version of this article:

Table S1. Genes differentially expressed in methimazole treated, spinal cord transected animals.

Table S2. Genes Differentially expressed in T3-treated, spinal cord transected animals.

Please note: As a service to our authors and readers, this journal provides supporting information supplied by the authors. Such materials are peer-reviewed and may be re-organized for online delivery, but are not copy-edited or typeset by Wiley-Blackwell. Technical support issues arising from supporting information (other than missing files) should be addressed to the authors.

Acknowledgements

The authors thank Dr Christine Gervasi for help in animal rearing and editorial comments, and the National Science Foundation (IOS 951043) and the New York State Spinal Cord Injury Research Trust (NYSPHS C020940) for support. We also thank Drs Nathaniel Heintz (Rockefeller University) and Virginia M.-Y. Lee (Univ. Penn.) for the BLBP and NF-M antibodies, respectively. Appreciation is also given to Chen Wang, Erica Hutchins and Yuanyuan Liu for their help with the figures and for their suggestions for improving the text.

Abbreviations

BLBP, brain lipid binding protein; CNS, central nervous system; MS-222, ethyl 3-aminobenzoate methanesulfonate; NF-M, middle neurofilament protein; NTS, neurotensin; PB, 0.1 M sodium phosphate, pH 7.4; qRT-PCR, quantitative real-time reverse transcriptase polymerase chain reaction; RMP, RNA polymerase II subunit 5-mediating protein; SOCS2, cytokine signaling 2; T3, 3,3′,5-triiodo-L-thyronine; TBS, Tris-buffered saline; TH, thyroid hormone.

References

Arber, S., Ladle, D.R., Lin, J.H., Frank, E. & Jessell, T.M. (2000) ETS gene Er81 controls the formation of functional connections between group Ia sensory afferents and motor neurons. *Cell*, **101**, 485–498.

Asch, W.S., Leake, D., Canger, A.K., Passini, M.A., Argenton, F. & Schechter, N. (1998) Cloning of zebrafish neurofilament cDNAs for plasticin and gefiltin: increased mRNA expression in ganglion cells after optic nerve injury. *J. Neurochem.*, **71**, 20–32.

Beattie, M.S., Bresnahan, J.C. & Lopate, G. (1990) Metamorphosis alters the response to spinal cord transection in *Xenopus laevis* frogs. *J. Neurobiol.*, **21**, 1108–1122.

Becker, T., Bernhardt, R.R., Reinhard, E., Wullimann, M.F., Tongiorgi, E. & Schachner, M. (1998) Readiness of zebrafish brain neurons to regenerate a spinal axon correlates with differential expression of specific cell recognition molecules. *J. Neurosci.*, **18**, 5789–5803.

Brown, D.D. & Cai, L. (2007) Amphibian metamorphosis. *Dev. Biol.*, **306**, 20–33.

Brown, D.D., Wang, Z., Kanamori, A., Eliceiri, B., Furlow, J.D. & Schwartzman, R. (1995) Amphibian metamorphosis: a complex program of gene expression changes controlled by the thyroid hormone. *Recent Prog. Horm. Res.*, **50**, 309–315.

Brown, D.D., Wang, Z., Furlow, J.D., Kanamori, A., Schwartzman, R.A., Remo, B.F. & Pinder, A. (1996) The thyroid hormone-induced tail resorption program during *Xenopus laevis* metamorphosis. *Proc. Natl. Acad. Sci. USA*, **93**, 1924–1929.

Buchholz, D.R., Heimeier, R.A., Das, B., Washington, T. & Shi, Y.B. (2007) Pairing morphology with gene expression in thyroid hormone-induced intestinal remodeling and identification of a core set of TH-induced genes across tadpole tissues. *Dev. Biol.*, **303**, 576–590.

Buckbinder, L. & Brown, D.D. (1993) Expression of the *Xenopus laevis* prolactin and thyrotropin genes during metamorphosis. *Proc. Natl. Acad. Sci. USA*, **90**, 3820–3824.

Consolazione, A., Milstein, C., Wright, B. & Cuello, A.C. (1981) Immunocytochemical detection of serotonin with monoclonal antibodies. *J. Histochem. Cytochem.*, **29**, 1425–1430.

Damjanovski, S., Ishizuya-Oka, A. & Shi, Y.B. (1999) Spatial and temporal regulation of collagenases-3, -4, and stromelysin -3 implicates distinct functions in apoptosis and tissue remodeling during frog metamorphosis. *Cell Res.*, **9**, 91–105.

Das, B., Heimeier, R.A., Buchholz, D.R. & Shi, Y.B. (2009) Identification of direct thyroid hormone response genes reveals the earliest gene regulation programs during frog metamorphosis. *J. Biol. Chem.*, **284**, 34167–34178.

Delgermaa, L., Hayashi, N., Dorjsuren, D., Nomura, T., Thuy le, T.T. & Murakami, S. (2004) Subcellular localization of RPB5-mediating protein and its putative functional partner. *Mol. Cell. Biol.*, **24**, 8556–8566.

Dent, J.N. (1962) Limb regeneration in larvae and metamorphosing individuals of the South African clawed toad. *J. Morphol.*, **110**, 61–77.

Denver, R.J. (2008) Chordate metamorphosis: ancient control by iodothyronines. *Curr. Biol.*, **18**, R567–R569.

Denver, R.J., Pavgi, S. & Shi, Y.B. (1997) Thyroid hormone-dependent gene expression program for *Xenopus* neural development. *J. Biol. Chem.*, **272**, 8179–8188.

Di Giovanni, S., Knights, C.D., Rao, M., Yakovlev, A., Beers, J., Catania, J., Avantaggiati, M.L. & Faden, A.I. (2006) The tumor suppressor protein p53 is required for neurite outgrowth and axon regeneration. *EMBO J.*, **25**, 4084–4096.

Dodd, M.H.I. & Dodd, J.M. (1976) The biology of metamorphosis. In Lofts, B. (Ed.), *Physiology of the Amphibia*. Academic Press, New York, pp. 467–576.

Etkin, W. & Gilbert, L.I. (1968) *Metamorphosis. A Problem in Developmental Biology.* Appleton-Century-Crofts, New York.

Feng, L., Hatten, M.E. & Heintz, N. (1994) Brain lipid-binding protein (BLBP): a novel signaling system in the developing mammalian CNS. *Neuron*, **12**, 895–908.

Forehand, C.J. & Farel, P.B. (1982) Anatomical and behavioral recovery from the effects of spinal cord transection: dependence on metamorphosis in anuran larvae. *J. Neurosci.*, **2**, 654–662.

Gervasi, C. & Szaro, B.G. (1997) Sequence and expression patterns of two forms of the middle molecular weight neurofilament protein (NF-M) of *Xenopus laevis*. *Brain Res. Mol. Brain Res.*, **48**, 229–242.

Gervasi, C., Thyagarajan, A. & Szaro, B.G. (2003) Increased expression of multiple neurofilament mRNAs during regeneration of vertebrate central nervous system axons. *J. Comp. Neurol.*, **461**, 262–275.

Gibbs, K.M. & Szaro, B.G. (2006) Regeneration of descending projections in *Xenopus laevis* tadpole spinal cord demonstrated by retrograde double labeling. *Brain Res.*, **1088**, 68–72.

Goldshmit, Y., Walters, C.E., Scott, H.J., Greenhalgh, C.J. & Turnley, A.M. (2004) SOCS2 induces neurite outgrowth by regulation of epidermal growth factor receptor activation. *J. Biol. Chem.*, **279**, 16349–16355.

Gudernatsch, J.F. (1912) Feeding experiments in Tadpoles. I. The influence of specific organs given as on growth and differentiation: a contribution to the knowledge of organs with internal secretion. *Arch. Ent.-mech. Org.*, **35**, 457–483.

Hasan, S.J., Keirstead, H.S., Muir, G.D. & Steeves, J.D. (1993) Axonal regeneration contributes to repair of injured brainstem-spinal neurons in embryonic chick. *J. Neurosci.*, **13**, 492–507.

Hasegawa, K., Chang, W.W., Li, H., Berlin, Y., Ikeda, O., Kane-Goldsmith, N. & Grumet, M. (2005) Embryonic radial glia bridge spinal cord lesions and promote functional recovery following spinal cord injury. *Exp. Neurol.*, **193**, 394–410.

Hevner, R.F., Daza, R.A., Rubenstein, J.L., Stunnenberg, H., Olavarria, J.F. & Englund, C. (2003) Beyond laminar fate: toward a molecular classification of cortical projection/pyramidal neurons. *Dev. Neurosci.*, **25**, 139–151.

Hoperskaya, O.A. (1975) The development of animals homozygous for a mutation causing periodic albinism (a^p) in *Xenopus laevis*. *J. Embryol. Exp. Morphol.*, **34**, 253–264.

Horlein, A.J., Naar, A.M., Heinzel, T., Torchia, J., Gloss, B., Kurokawa, R., Ryan, A., Kamei, Y., Soderstrom, M. & Glass, C.K. (1995) Ligand-independent repression by the thyroid hormone receptor mediated by a nuclear receptor co-repressor. *Nature*, **377**, 397–404.

Howdeshell, K.L. (2002) A model of the development of the brain as a construct of the thyroid system. *Environ. Health Perspect.*, **110**(Suppl. 3), 337–348.

Hutson, L.D. & Bothwell, M. (2001) Expression and function of *Xenopus laevis* p75(NTR) suggest evolution of developmental regulatory mechanisms. *J. Neurobiol.*, **49**, 79–98.

Jacobs, A.J., Swain, G.P., Snedeker, J.A., Pijak, D.S., Gladstone, L.J. & Selzer, M.E. (1997) Recovery of neurofilament expression selectively in regenerating reticulospinal neurons. *J. Neurosci.*, **17**, 5206–5220.

Jacobson, R.D., Virag, I. & Skene, J.H. (1986) A protein associated with axon growth, GAP-43, is widely distributed and developmentally regulated in rat CNS. *J. Neurosci.*, **6**, 1843–1855.

Johnson, K.G., McKinnell, I.W., Stoker, A.W. & Holt, C.E. (2001) Receptor protein tyrosine phosphatases regulate retinal ganglion cell axon outgrowth in the developing *Xenopus* visual system. *J. Neurobiol.*, **49**, 99–117.

Knerlich-Lukoschus, F., Juraschek, M., Blomer, U., Lucius, R., Mehdorn, H.M. & Held-Feindt, J. (2008) Force-dependent development of neuropathic central pain and time-related CCL2/CCR2 expression after graded spinal cord contusion injuries of the rat. *J. Neurotrauma*, **25**, 427–448.

Kollros, J.J. (1981) Transitions in the nervous system during amphibian metamorphosis. In Gilbert, L.I. & Frieden, E. (Eds), *Metamorphosis: A Problem in Developmental Biology.* Plenum Press, New York, pp. 445–459.

Lancaster, C.A., Taylor-Harris, P.M., Self, A.J., Brill, S., van Erp, H.E. & Hall, A. (1994) Characterization of rhoGAP. A GTPase-activating protein for rho-related small GTPases. *J. Biol. Chem.*, **269**, 1137–1142.

Leloup, J. & Buscaglia, M. (1977) La triiodothyronine, hormone de la metamorphose des Amphibiens. *C. R. Acad. Sci*, **284**, 2261–2263.

Lin, W. & Szaro, B.G. (1994) Maturation of neurites in mixed cultures of spinal cord neurons and muscle cells from *Xenopus laevis* embryos followed with antibodies to neurofilament proteins. *J. Neurobiol.*, **25**, 1235–1248.

Livak, K.J. & Schmittgen, T.D. (2001) Analysis of relative gene expression data using real-time quantitative PCR and the $2^{-\Delta\Delta CT}$ method. *Methods*, **25**, 402–408.

Marsh-Armstrong, N., Cai, L. & Brown, D.D. (2004) Thyroid hormone controls the development of connections between the spinal cord and limbs during *Xenopus laevis* metamorphosis. *Proc. Natl. Acad. Sci. USA*, **101**, 165–170.

Mazella, J., Zsurger, N., Navarro, V., Chabry, J., Kaghad, M., Caput, D., Ferrara, P., Vita, N., Gully, D., Maffrand, J.P. & Vincent, J.P. (1998) The 100-kDa neurotensin receptor is gp95/sortilin, a non-G-protein-coupled receptor. *J. Biol. Chem.*, **273**, 26273–26276.

Michel, M.E. & Reier, P.J. (1979) Axonal-ependymal associations during early regeneration of the transected spinal cord in *Xenopus laevis* tadpoles. *J. Neurocytol.*, **8**, 529–548.

van Mier, P. & Ten Donkelaar, H.J. (1984) Early development of descending pathways from the brain stem to the spinal cord in *Xenopus laevis*. *Anat. Embryol. (Berl.)*, **170**, 295–306.
van Mier, P., Joosten, H.W., van Rheden, R. & Ten Donkelaar, H.J. (1986) The development of serotonergic raphespinal projections in *Xenopus laevis*. *Int. J. Dev. Neurosci.*, **4**, 465–475.
Milstein, C., Wright, B. & Cuello, A.C. (1983) The discrepancy between the cross-reactivity of a monoclonal antibody to serotonin and its immunohistochemical specificity. *Mol. Immunol.*, **20**, 113–123.
Muchow, M., Bossis, I. & Porter, T.E. (2005) Ontogeny of pituitary throtrophs and regulation by endogenous thryoid hormone feedback in the chick embryo. *J. Endocrinol.*, **184**, 407–416.
Nakanishi, H. (2003) Microglial functions and proteases. *Mol. Neurobiol.*, **27**, 163–176.
Nieuwkoop, P.D. & Faber, J. (1994) *Normal Table of Xenopus laevis* (Daudin). Garland, New York.
Norris, C.R. & Kalil, K. (1991) Guidance of callosal axons by radial glia in the developing cerebral cortex. *J. Neurosci.*, **11**, 3481–3492.
Nykjaer, A., Lee, R., Teng, K.K., Jansen, P., Madsen, P., Nielsen, M.S., Jacobsen, C., Kliemannel, M., Schwarz, E., Willnow, T.E., Hempstead, B.L. & Petersen, C.M. (2004) Sortilin is essential for proNGF-induced neuronal cell death. *Nature*, **427**, 843–848.
Paulsen, S.J., Larsen, L.K., Jelsing, J., Janssen, U., Gerstmayer, B. & Vrang, N. (2009) Gene expression profiling of individual hypothalamic nuclei from single animals using laser capture microdissection and microarrays. *J. Neurosci. Methods*, **177**, 87–93.
Piessevaux, J., Lavens, D., Montoye, T., Wauman, J., Catteeuw, D., Vandekerckhove, J., Belsham, D., Peelman, F. & Tavernier, J. (2006) Functional cross-modulation between SOCS proteins can stimulate cytokine signaling. *J. Biol. Chem.*, **281**, 32953–32966.
Raymond, P.A., Barthel, L.K., Bernardos, R.L. & Perkowski, J.J. (2006) Molecular characterization of retinal stem cells and their niches in adult zebrafish. *BMC Dev. Biol.*, **6**, 36.
Rehermann, M.I., Marichal, N., Russo, R.E. & Trujillo-Cenoz, O. (2009) Neural reconnection in the transected spinal cord of the freshwater turtle *Trachemys dorbignyi*. *J. Comp. Neurol.*, **515**, 197–214.
Sachs, L. (1984) *Applied Statistics: A Handbook of Techniques*. Springer-Verlag, New York.
Saunders, N.R., Balkwill, P., Knott, G., Habgood, M.D., Mollgard, K., Treherne, J.M. & Nicholls, J.G. (1992) Growth of axons through a lesion in the intact CNS of fetal rat maintained in long-term culture. *Proc. Biol. Sci.*, **250**, 171–180.
Shaw, G. (1992) A neurofilament-specific sequence motif. *Trends Biochem. Sci.*, **17**, 3405.
Shi, Y.B. (2000) *Amphibian Metamorphosis: From Morphology to Molecular Biology*. Wiley-Liss, New York.
Shi, Y.B. (2009) Dual functions of thyroid hormone receptors in vertebrate development: the roles of histone-modifying cofactor complexes. *Thyroid*, **19**, 987–999.
Shi, Y.B. & Brown, D.D. (1993) The earliest changes in gene expression in tadpole intestine induced by thyroid hormone. *J. Biol. Chem.*, **268**, 20312–20317.
Simon, R., Tietge, J.E., Michalke, B., Degitz, S. & Schramm, K.W. (2002) Iodine species and the endocrine system: thyroid hormone levels in adult *Danio rerio* and developing *Xenopus laevis*. *Anal. Bioanal. Chem.*, **372**, 481–485.
Sims, R.T. (1962) Transection of the spinal cord in developing *Xenopus laevis*. *J. Embryol. Exp. Morphol.*, **10**, 115–126.
Singer, M., Nordlander, R.H. & Egar, M. (1979) Axonal guidance during embryogenesis and regeneration in the spinal cord of the newt: the blueprint hypothesis of neuronal pathway patterning. *J. Comp. Neurol.*, **185**, 1–21.
Skene, J.H., Jacobson, R.D., Snipes, G.J., McGuire, C.B., Norden, J.J. & Freeman, J.A. (1986) A protein induced during nerve growth (GAP-43) is a major component of growth-cone membranes. *Science*, **233**, 783–786.
St.Germain, D.L., Schwartzman, R.A., Croteau, W., Kanamori, A., Wang, Z., Brown, D.D. & Galton, V.A. (1994) A thyroid hormone-regulated gene in *Xenopus laevis* encodes a type III iodothyronine 5-deiodinase. *Proc. Natl. Acad. Sci. USA*, **91**, 7767–7771.
Szaro, B.G. & Gainer, H. (1988) Immunocytochemical identification of non-neuronal intermediate filament proteins in the developing *Xenopus laevis* nervous system. *Brain Res. Dev. Brain Res.*, **43**, 207–224.
Szaro, B.G., Lee, V.M. & Gainer, H. (1989) Spatial and temporal expression of phosphorylated and non-phosphorylated forms of neurofilament proteins in the developing nervous system of *Xenopus laevis*. *Brain Res. Dev. Brain Res.*, **48**, 87–103.
Takahashi, K., Yoshida, N., Murakami, N., Kawata, K., Ishizaki, H., Tanaka-Okamoto, M., Miyoshi, J., Zinn, A.R., Shime, H. & Inoue, N. (2007) Dynamic regulation of p53 subnuclear localization and senescence by MORC3. *Mol. Biol. Cell*, **18**, 1701–1709.
Takeda, A., Goris, R.C. & Funakoshi, K. (2007) Regeneration of descending projections to the spinal motor neurons after spinal hemisection in the goldfish. *Brain Res.*, **1155**, 17–23.
Tata, J.R. (2006) Amphibian metamorphosis as a model for the developmental actions of thyroid hormone. *Mol. Cell. Endocrinol.*, **246**, 10–20.
Taylor, J.S.H., Jack, J.L. & Easter, S.S. Jr (1989) Is the capacity for optic nerve regeneration related to continued retinal ganglion cell production in the frog? A test of the hypothesis that neurogenesis and axon regeneration are obligatorily linked. *Eur. J. Neurosci.*, **1**, 626–638.
Ten Donkelaar, H.J. (2000) Development and regenerative capacity of descending supraspinal pathways in tetrapods: a comparative approach. *Adv. Anat. Embryol. Cell Biol.*, **154**, 1–145.
Tompkins, R. (1977) Grafting analysis of the periodic albino mutant of *Xenopus laevis*. *Dev. Biol.*, **57**, 460–464.
Undamatla, J. & Szaro, B.G. (2001) Differential expression and localization of neuronal intermediate filament proteins within newly developing neurites in dissociated cultures of *Xenopus laevis* embryonic spinal cord. *Cell Motil. Cytoskeleton*, **49**, 16–32.
Wang, Z. & Brown, D.D. (1993) Thyroid hormone-induced gene expression program for amphibian tail resorption. *J. Biol. Chem.*, **268**, 16270–16278.
Weiss, P. & Rosetti, F. (1951) Growth responses of opposite sign among different neuron types exposed to thyroid hormone. *Proc. Natl. Acad. Sci. USA*, **37**, 540–546.
Wetzel, D.M., Lee, V.M. & Erulkar, S.D. (1989) Long-term cultures of neurons from adult frog brain express GABA and glutamate-activated channels. *J. Neurobiol.*, **20**, 255–270.
Will, U. (1986) Mauthner neurons survive metamorphosis in anurans: a comparative HRP study on the cytoarchitecture of Mauthner neurons in amphibians. *J. Comp. Neurol.*, **244**, 111–120.
Yoshida, K., Suzuki, Y., Yamamoto, K. & Sinohara, H. (1999) cDNA sequencing of guinea pig alpha 2-HS glycoprotein, its expression in various tissues and acute phase expression. *Biol. Chem.*, **380**, 95–99.
Zhang, L. & McClellan, A.D. (1999) Axonal regeneration of descending brain neurons in larval lamprey demonstrated by retrograde double labeling. *J. Comp. Neurol.*, **410**, 612–626.
Zhang, S., Xia, Y.Y., Lim, H.C., Tang, F.R. & Feng, Z.W. (2010) NCAM-mediated locomotor recovery from spinal cord contusion injury involves neuroprotection, axon regeneration, and synaptogenesis. *Neurochem. Int.*, **56**, 919–929.
Zhao, Y. & Szaro, B.G. (1994) The return of phosphorylated and nonphosphorylated epitopes of neurofilament proteins to the regenerating optic nerve of *Xenopus laevis*. *J. Comp. Neurol.*, **343**, 158–172.
Zottoli, S.J. & Freemer, M.M. (2006) Recovery of **C**-starts, equilibrium and targeted feeding after whole spinal cord crush in the adult goldfish *Carassius auratus*. *J. Exp. Biol.*, **206**, 3015–3029.